MAGELLAN: Autonomous Cross-Disciplinary Scientific Hypothesis Generation via Adversarial Multi-Agent Systems

Alberto Trivero
Kakashi Venture Accelerator
Torino, Italy
alberto@kakashi.ventures
https://magellan-discover.ai

Abstract

We present MAGELLAN, an open-source multi-agent system built on Claude Code (Anthropic) that autonomously generates cross-disciplinary scientific hypotheses by connecting fields that lack mutual citation. Building on Swanson's "Undiscovered Public Knowledge" principle (1986), MAGELLAN replaces bibliometric methods with frontier large language models (Claude Opus 4.6 and Sonnet 4.6) that have absorbed the literature of multiple disciplines. The system comprises 15 specialized agents: a Scout that autonomously identifies promising cross-field bridges using 10 formalized strategies, a Generator that creates hypotheses from parametric knowledge, and an adversarial pipeline (Critic with 9 attack vectors, Quality Gate with ∼60% rejection rate, independent validation by GPT-5.4 Pro and Gemini 3.1 Pro) that systematically eliminates weak candidates.

Over 22 sessions, MAGELLAN generated 273 hypotheses, of which 102 (37%) survived the full adversarial pipeline. Surviving hypotheses are not surface analogies: they involve first-principles derivations from physical theorems applied to new biological domains, quantitative predictions with specific falsification experiments, and the kind of cross-disciplinary reasoning that would require years of cross-training for a human researcher. We verify two hypotheses at different levels of a validation taxonomy: (1) applying extreme value theory to the Meltome Atlas (48,000 proteins, 13 species)—the first such application, producing novel findings (universal Weibull-domain behavior, measurement censoring diagnostic) despite failing to confirm the predicted correlation with growth temperature; (2) deriving the Cramér-Rao bound for plant gravitropic sensing from published statolith parameters—a mathematical derivation confirmed from first principles, showing plants operate 1–6× above the fundamental physical limit. A third hypothesis (percolation theory for tumor immune exclusion) has independent convergence evidence from a clinical trial, a patent, and a peer-reviewed publication. Meta-learning across sessions reveals that mathematical constraints transfer more reliably than analogies, fully disjoint field pairs produce substantially better hypotheses (84% vs. 30% survival), and the bottleneck in AI-assisted discovery has shifted from hypothesis generation to domain expertise for evaluation.

Unlike proprietary systems (Google AI Co-Scientist, FutureHouse), MAGELLAN is fully open-source (Apache 2.0), fully autonomous in target selection, and publishes all results as CC0 public domain. Code, hypotheses, methodology, and computational verifications are publicly available.

1 Introduction

In 1986, Don Swanson articulated a problem that remains central to scientific progress: the literature contains logical connections that no researcher has made—not because the evidence is missing, but

because it resides in *disjoint literatures* that never cite each other (Swanson, 1986). Swanson's canonical example linked dietary fish oil to Raynaud's disease through eleven intermediate concepts scattered across the hematology and nutrition literatures. Both fields were individually well-studied; neither community cited the other. He termed this phenomenon *Undiscovered Public Knowledge* (UPK) and formalized it as the ABC model: Field A and Field C share an intermediate concept B (the *bridge term*) that appears in both, but A and C lack mutual citation. Discovery consists of identifying B and constructing the inference $A \rightarrow B \rightarrow C$.

Four decades later, the problem has intensified by orders of magnitude. PubMed indexes over 36 million articles, with approximately 1.5 million added per year. The average biomedical researcher reads roughly 250 papers annually (Tenopir et al., 2009). A tumor immunologist is unlikely to encounter percolation theory from statistical physics; a plant biologist measuring statolith sedimentation is unlikely to recognize that the Cramér-Rao bound from estimation theory applies to their system. The connections exist in the published record but remain undiscovered—victims of disciplinary silos that grow deeper as the literature grows larger. Swanson's insight was prescient: the rate of knowledge production has outpaced the rate of knowledge integration, and the gap is widening.

Swanson's original method for finding UPK was *bibliometric*: co-occurrence analysis of MeSH terms, citation graph traversal, and frequency matrices. Systems like Arrowsmith (Smalheiser, 2009), BITOLA (Hristovski et al., 2006), and subsequent Literature-Based Discovery (LBD) tools refined this approach over three decades. These methods remain valuable for structured, high-throughput identification of candidate bridge terms. However, they are fundamentally limited to connections that leave statistical traces in the citation graph—they cannot discover structural isomorphisms, mathematical analogies, or physical-law constraints that cross disciplinary boundaries without shared terminology.

1.1 Large Language Models as Universal Readers

Large language models (LLMs) offer a qualitatively different approach. Models trained on broad scientific corpora have, in a meaningful sense, "read" the literatures of multiple fields simultaneously. Frontier models (March 2026) score 91–94% on GPQA Diamond—PhD-level questions spanning biology, physics, and chemistry (Rein et al., 2023)—a 55-point improvement over GPT-4's 39% in 2023. This represents not merely improved question-answering but a demonstrated capacity for deep cross-disciplinary reasoning. The UPK problem exists because no individual researcher can read both literatures; an LLM has absorbed both.

This observation suggests a paradigm shift: the problem is no longer *detecting citation disjunction* (bibliometric methods) but *eliciting latent connections* from a model that already contains the knowledge of both fields. The evidence supports this reframing: none of the AI-driven scientific breakthroughs of 2025–2026—including GPT-5's collaboration with Ginkgo Bioworks on cell-free protein synthesis (Ginkgo Bioworks, 2026), Google AI Co-Scientist's experimentally validated discoveries (Gottweis et al., 2025), and DeepMind Aletheia's solutions to open Erdős problems (DeepMind, 2025)—used bibliometric analysis. All employed parametric knowledge combined with multi-agent architecture and debate or evolution.

1.2 The Hallucination Problem

However, LLMs also hallucinate, confabulate citations, and produce fluent nonsense (Ji et al., 2023). On open factual recall (AA-Omniscience benchmark), the best frontier model reaches only 55% accuracy on the raw accuracy metric; the benchmark's primary Omniscience Index (scaled -100 to $+100$,

penalizing hallucinated confidence) reaches only 33. Hallucination rates range from 22% to 48% depending on model and benchmark. On the FrontierScience-Research benchmark (open research tasks), GPT-5.2 achieves only 25.3%—a 52-point gap below its 77% on structured tasks (OpenAI, 2025). These numbers make clear that the challenge in AI-driven scientific discovery is not *generation* but *filtration*: separating genuine cross-disciplinary insights from plausible-sounding artifacts.

This problem is compounded by a subtler failure mode. Si et al. (Si et al., 2025a) found that LLM-generated research ideas score *higher* on novelty than human ideas during blind expert review (5.6 vs. 4.8 on a 10-point scale). However, a follow-up study executing these ideas experimentally (Si & Hashimoto, 2025) revealed that overall quality drops sharply after testing: LLM ideas fell from 5.4 to 3.4, while human ideas declined less (4.6 to 4.0). The implication is that LLM-generated "novelty" may partly be an artifact of incorrect parametric knowledge—ideas that *appear* new because they are *wrong* in non-obvious ways. Any system that claims to generate scientific hypotheses must confront this head-on.

The challenge of evaluating AI-generated science is increasingly well-benchmarked. Beyond GPQA Diamond and FrontierScience-Research, recent benchmarks include Humanity's Last Exam (Phan et al., 2025) (2,500 expert-crafted questions where the best model scores ∼18%, published in *Nature*), DiscoveryBench (Majumder et al., 2024) (hypothesis-driven data analysis tasks), and ResearchBench (Liu et al., 2025) (end-to-end research evaluation). These benchmarks consistently show that structured question-answering performance far outpaces open-ended scientific reasoning.

Skeptical assessments reinforce this gap. A December 2025 review of AI-generated materials science claims found "scant evidence for compounds that fulfill the trifecta of novelty, credibility, and utility," concluding that many AI-discovered materials had been previously known or were not synthesizable. Similarly, claims in October 2025 that GPT-5 had solved previously unsolved mathematical problems were subsequently revealed to be rediscoveries of known results. These episodes underscore the importance of rigorous adversarial filtration and external validation.

1.3 The MAGELLAN Approach

MAGELLAN (**M**ulti-**A**gent **G**enerative **E**xploration of **L**atent **L**inks **A**cross k**N**owledge) addresses these challenges through three design principles:

Parametric generation + retrieval validation. The LLM's parametric knowledge is the *generative engine*—the source of non-obvious cross-disciplinary connections. But every factual claim is verified through external retrieval (PubMed, Semantic Scholar, KEGG, STRING, and web search). Neither parametric-only (hallucination risk) nor retrieval-only (misses novel connections) suffices; the combination is essential. MOOSE-Chem (Yang et al., 2024b) provides independent evidence for this paradigm, demonstrating that LLMs encode "latent scientific knowledge associations not yet recognized by humans." TruthHypo (Xiong et al., 2025) provides the complementary evidence: LLMs struggle with truthful hypothesis generation without grounding support.

Adversarial multi-agent architecture. Rather than trusting a single model's output, MAGELLAN sets 15 specialized agents against each other. A Generator proposes hypotheses; a Critic attacks them with 9 adversarial vectors including claim-level fact verification; a Quality Gate applies a 10-point rubric and rejects approximately 60% of candidates; independent external models (GPT-5.4 Pro, Gemini 3.1 Pro) attempt to break what survives. The design principle is that *being wrong less often* matters more than being creative more often.

Autonomous target selection. Unlike most comparable systems, which require a scientist-in-the-loop to frame the research question, MAGELLAN's Scout agent autonomously decides *where* to look—which pairs of fields to connect, through which bridge mechanisms. This is a more ambitious capability claim than hypothesis generation alone: the system must identify not just answers but questions.

1.4 Contributions

Our contributions are:

1. An open-source, 15-agent system for fully autonomous cross-disciplinary hypothesis generation, combining parametric generation with adversarial retrieval validation and cross-model verification. The system is released under Apache 2.0; all discovery outputs from autonomous mode are released as CC0 (public domain).

2. Quantitative evaluation over 22 sessions (273 hypotheses generated, 102 surviving the full adversarial pipeline at a 37% survival rate), with detailed analysis of strategy performance, bridge type survival rates, and the effect of citation disjointness on hypothesis quality.

3. Two computational verifications on public data demonstrating that surviving hypotheses involve genuine first-principles reasoning, not surface analogies: (a) applying extreme value theory to the Meltome Atlas (48,000 proteins, 13 species)—the first such application, revealing universal Weibull-domain behavior but failing to confirm the predicted correlation with growth temperature due to measurement censoring; and (b) deriving the Cramér-Rao bound for plant gravitropic sensing from published statolith parameters—a mathematical derivation from first principles that is confirmed by published measurements, showing plants operate 1–6× above the fundamental physical limit. Both analyses had zero prior literature: the system autonomously connected fields that no human researcher had bridged, producing derivations that would require simultaneous expertise in statistical physics and the respective biological domains.

4. A meta-learning framework that accumulates strategy performance data, bridge type survival rates, and kill pattern analysis across sessions, enabling the system to improve its target selection over time.

2 Related Work

Scientific hypothesis generation by AI systems has a history extending from Swanson's bibliometric methods through knowledge-graph-based approaches to the current generation of LLM-powered multi-agent systems. We organize the landscape by approach, summarize each system's capabilities and limitations, and position MAGELLAN relative to the state of the art.

2.1 Bibliometric and Literature-Based Discovery

Swanson's foundational work (Swanson, 1986, 1988) demonstrated that co-occurrence analysis of MeSH terms and citation graphs could identify previously unlinked literatures. His fish oil–Raynaud's disease and magnesium–migraine predictions were subsequently confirmed by clinical trials, establishing that Undiscovered Public Knowledge is a real and actionable phenomenon.

Subsequent systems—Arrowsmith (Smalheiser, 2009), BITOLA (Hristovski et al., 2006), and more recent automated LBD tools—refined the bibliometric approach with improved statistical

methods and larger corpora. These systems remain valuable for high-throughput screening of candidate bridge terms within structured bibliographic databases. However, they are inherently limited to connections that leave statistical traces in the citation graph: shared MeSH terms, co-cited references, or overlapping author networks. Structural isomorphisms (e.g., percolation theory connecting epidemiology and fracture mechanics), mathematical analogies (e.g., the Cramér-Rao bound applying to both neural sensory coding and plant gravitropism), and physical-law constraints (e.g., the thermodynamic uncertainty relation bounding bacterial cell-size control) cross disciplinary boundaries without shared terminology and are invisible to bibliometric methods.

2.2 Knowledge-Graph-Based Approaches

SciAgents (Ghafarollahi & Buehler, 2024) represents the most developed KG-based approach, employing an Ontologist, multiple Scientist agents, and a Critic operating over a persistent knowledge graph of 33,000+ nodes. The system discovers cross-disciplinary connections by sampling paths through the graph, grounding hypotheses in explicit ontological relationships. The persistent KG provides structural advantages: multi-hop reasoning across accumulated knowledge and explicit relationship typing. However, the approach requires substantial upfront investment in graph construction and maintenance, and the quality of discoveries is bounded by the coverage and currency of the graph.

2.3 LLM-Powered Multi-Agent Systems

The 2025–2026 period has seen a proliferation of multi-agent systems for scientific discovery, each making different architectural choices along the axes of autonomy, validation rigor, and openness.

Google AI Co-Scientist. Gottweis et al. (Gottweis et al., 2025) demonstrated multi-agent scientific reasoning with six agents on Gemini 2.0 using Elo-based tournament ranking. The system produced three experimentally validated discoveries: KIRA6 for acute myeloid leukemia, vorinostat for hepatic fibrosis (published in *Advanced Science*), and cf-PICIs for bacterial gene transfer (published in *Cell*—notably a recapitulation of findings that researchers had spent approximately a decade validating, rather than a de novo discovery). A partnership with the U.S. Department of Energy extended the system to 17 National Laboratories. Critically, AI Co-Scientist requires a scientist-in-the-loop to frame the research question—the system generates hypotheses *within* a human-defined problem space but does not autonomously identify which problems to investigate.

FutureHouse / Kosmos. Edison Scientific, FutureHouse's for-profit spinout, raised $70M (led by Spark Capital at ∼$250M valuation, December 2025) and developed Kosmos (Mitchener et al., 2025), a system achieving 79.4% overall accuracy on structured agentic tasks with 12-hour execution runs generating up to 42,000 lines of code and processing 1,500 papers. However, accuracy on novel synthesis and interpretation tasks drops to 57.9%, and the developers note that the system "often goes down rabbit holes." Kosmos is partially open-source. Like AI Co-Scientist, it receives human-defined research objectives rather than autonomously selecting targets.

Sakana AI Scientist v2. Lu et al. (Lu et al., 2024) demonstrated end-to-end paper generation including ideation, experimentation, and writing, producing an AI-authored paper accepted at an ICLR 2025 workshop (subsequently withdrawn per a pre-registered protocol). The broader methodology was later published in *Nature* (March 2026). The system focuses on machine learning

research—generating and executing experiments within ML—rather than cross-disciplinary hypothesis generation in the natural sciences. Its primary contribution is demonstrating that AI systems can produce publishable research artifacts, albeit within a narrow domain.

POPPER. Huang et al. (Huang et al., 2025) implemented falsification-based hypothesis refinement with Type-I error control comparable to human scientists at 10× speed. POPPER's emphasis on falsification aligns with MAGELLAN's adversarial pipeline, but POPPER operates within a given hypothesis space rather than autonomously identifying cross-disciplinary targets. The system provides strong evidence that LLM-based agents can maintain statistical rigor in hypothesis evaluation.

Virtual Lab. The Virtual Lab system (Swanson et al., 2024) employs a principal investigator agent coordinating multiple scientist agents to design nanobodies, producing 92 candidates of which 2 showed improved binding affinity in wet-lab validation. This represents one of the few systems with experimental validation of AI-generated molecular designs. However, Virtual Lab operates within protein engineering rather than cross-disciplinary hypothesis generation, and the PI agent receives the research objective from a human user.

MOOSE-Chem. Yang et al. (Yang et al., 2024b) demonstrated that LLMs encode "latent scientific knowledge associations not yet recognized by humans," providing direct empirical support for the UPK thesis applied to language models. MOOSE-Chem focuses on chemistry and uses inspiration papers to guide hypothesis generation, requiring human curation of seed literature.

TruthHypo. Xiong et al. (Xiong et al., 2025) showed that LLMs struggle with truthful hypothesis generation without grounding support, finding significant rates of factually incorrect claims in ungrounded hypotheses. This work validates the parametric-generation + retrieval-validation paradigm: parametric knowledge is necessary for creative cross-disciplinary connections, but retrieval is necessary for factual accuracy.

AlphaEvolve. DeepMind's AlphaEvolve (DeepMind, 2025b) uses an evolutionary coding agent powered by Gemini to discover novel algorithms, most notably improving 4×4 matrix multiplication for the first time in 56 years (in collaboration with Terence Tao). Unlike hypothesis-generation systems, AlphaEvolve discovers *procedures* rather than scientific hypotheses, but its success demonstrates that LLMs can find genuinely novel results in well-defined combinatorial search spaces.

Agent Laboratory. Schmidgall et al. (Schmidgall et al., 2025) proposed a multi-agent framework for end-to-end research, from literature review through experimentation to paper writing, with NeurIPS-style evaluation metrics. The system demonstrated that AI agents can coordinate across research phases, though it focuses on ML experiments rather than cross-disciplinary natural science.

Other systems. Several additional multi-agent systems have been developed for scientific tasks, including NovelSeek (closed-loop multi-agent discovery with iterative refinement) and AstroAgents (8-agent system for astrophysics hypothesis generation, architecturally comparable to MAGELLAN in agent count and specialization). A comprehensive taxonomy is provided by Li et al. (Li et al., 2025), who classify AI scientists along a six-stage research pipeline (problem identification, hypothesis generation, experiment design, experimentation, result analysis, reporting).

Table 1: Comparison of AI scientific discovery systems (as of March 2026). "Target Autonomy" indicates whether the system autonomously selects research targets or requires human-defined objectives. "Validation" describes the primary method for filtering or verifying hypotheses. "Open" indicates source code availability. "Published Results" indicates whether generated hypotheses or discoveries have been made publicly available with sufficient detail for independent evaluation.

System	Target Autonomy	Validation	Open	Published Results	Domain
Swanson / Arrowsmith	Manual	Bibliometric	Yes	Yes	Biomedicine
SciAgents	Manual	KG paths + Critic	Yes	Partial	Cross-domain
Google AI Co-Scientist	Human-in-loop	Elo tournament	No	3 validated	Biomedicine
FutureHouse / Kosmos	Human-defined	Multi-agent	Partial	Partial	Biomedicine
Sakana AI Scientist v2	Semi-auto (ML)	Peer review sim.	Yes	Yes (ML)	Machine Learning
POPPER	Human-defined	Falsification	Yes	Yes	General
Virtual Lab	Human-defined	Wet-lab testing	Partial	Yes (nanobodies)	Protein eng.
MOOSE-Chem	Human-curated	Inspiration papers	Yes	Yes	Chemistry
TruthHypo	Human-defined	Grounding check	Yes	Yes	General
AlphaEvolve	Semi-auto	Evolutionary	Partial	Yes (algorithms)	Mathematics
Agent Laboratory	Human-defined	Multi-agent	Yes	Yes (ML)	Machine Learning
Aletheia	Semi-auto (math)	Verifier-Reviser	No	Partial (4 proofs)	Mathematics
MAGELLAN	**Fully autonomous**	**Adversarial + cross-model**	**Yes**	**Yes (273 hyps.)**	**Life sciences**

Aletheia. DeepMind's Aletheia system (DeepMind, 2025) employs a Generator-Verifier-Reviser architecture on Gemini Deep Think, solving 4 open Erdős problems and 6 of 10 FirstProof challenge problems autonomously. However, of 200 evaluable solution candidates (filtered from 700 open problems attempted), the system produces errors in 68.5% of cases, underscoring the difficulty of reliable autonomous reasoning even for frontier models. Aletheia is not open-source and focuses on pure mathematics rather than cross-disciplinary natural science.

2.4 Comparison

Viewed collectively, the systems above reveal a consistent pattern: the field has made rapid progress on hypothesis *generation* and *evaluation within defined problem spaces*, but two capabilities remain largely unaddressed. First, **autonomous target selection**—deciding *what* to investigate without human guidance—is absent from nearly every system. Google AI Co-Scientist, POPPER, Virtual Lab, MOOSE-Chem, and Agent Laboratory all require a scientist to frame the research question. Second, **cross-disciplinary connections that cross terminological boundaries**—structural isomorphisms, mathematical analogies, physical-law constraints—are invisible to both bibliometric methods and keyword-based retrieval. No published system systematically searches for these. MAGELLAN is designed to address both gaps simultaneously: the Scout autonomously identifies cross-field targets, and the parametric-generation paradigm elicits connections that share no common vocabulary between fields.

Table 1 summarizes the landscape along six axes that we consider critical for evaluating scientific discovery systems: target autonomy (does the system choose what to investigate?), validation methodology, openness, whether results have been published, the primary knowledge source, and the domain of operation.

Several observations emerge from this comparison. First, MAGELLAN is among the very few systems that autonomously selects research targets. Demis Hassabis has stated that systems capable of "not only solving an important problem in science but coming up with it in the first place" are 5–10 years away (CBS *60 Minutes*, April 20, 2025). MAGELLAN's Scout represents an early attempt at this capability, with the caveat that selecting *promising* cross-disciplinary targets is easier than selecting *important* ones—a distinction we do not claim to have resolved.

Second, MAGELLAN's adversarial validation pipeline (9 Critic attack vectors, 10-point Quality Gate rubric, cross-model validation by GPT-5.4 Pro and Gemini 3.1 Pro) is among the most elaborate, though Google AI Co-Scientist's Elo tournament and POPPER's falsification framework are comparably rigorous within their respective scopes.

Third, most systems are either proprietary (Google AI Co-Scientist, Aletheia) or publish results selectively. MAGELLAN publishes all hypotheses, methodology, and code under Apache 2.0 / CC0, enabling independent evaluation and reproduction.

Known gaps relative to the state of the art. MAGELLAN lacks a persistent knowledge graph (cf. SciAgents' 33,000+ node KG), does not run in silico scientific simulations (cf. Virtual Lab's molecular dynamics), uses Elo tournament ranking only as a diagnostic sanity check rather than as the primary ranking method (cf. AI Co-Scientist), and has no experimentally validated discoveries (cf. AI Co-Scientist's three lab-confirmed results, Virtual Lab's two validated nanobodies). We consider the absence of experimental validation the most significant limitation and discuss it further in Section 6.

3 System Architecture

MAGELLAN comprises 15 specialized agents coordinated by an Orchestrator that functions as a pure dispatcher (Table 2). The Orchestrator has no web search capability and cannot execute pipeline phases inline—it must delegate every phase to the appropriate sub-agent. This is a deliberate architectural constraint, not a limitation: early prototypes allowed the Orchestrator to reason about hypotheses directly, which led to it rationalizing weak hypotheses rather than subjecting them to adversarial review. Removing web search tools from the Orchestrator enforces separation of concerns—coordination logic cannot contaminate evaluation logic. A dispatch log (`state/dispatch-log.json`) records every agent invocation with timestamps for post-session audit.

The pipeline proceeds through three phases: *Exploration* (target identification and validation), *Generation & Critique* (hypothesis creation, adversarial evaluation, ranking, and evolution over 1–3 adaptive cycles), and *Final Validation & Meta-Learning* (quality gate, cross-model validation, empirical evidence mining, and session analysis). We describe each phase and its constituent agents in the subsections below.

3.1 Implementation: Claude Code as Foundation

MAGELLAN is not a standalone application—it is built entirely on **Claude Code** (Anthropic's agentic coding CLI), which serves as both the execution platform and the architectural foundation. Claude Code provides the capabilities that make a 15-agent adversarial pipeline possible without custom infrastructure: agent dispatch and lifecycle management (spawning sub-agents with per-agent model and effort configuration), tool access control (restricting which tools each agent can use—e.g., removing web search from the Orchestrator), hook-based quality enforcement (SubagentStop hooks that deterministically validate outputs before completion), Model Context Protocol (MCP) integration for structured data retrieval, persistent file-based state management, and slash commands for user interaction (`/discover`, `/validate`, `/status`).

The choice of Claude Code was motivated by two factors: (1) it is the only agentic platform (as of March 2026) that supports hierarchical multi-agent dispatch with per-agent model selection, tool restriction, and deterministic output validation hooks, and (2) it enables the entire system—agents,

prompts, hooks, and configuration—to be version-controlled and open-sourced as a single repository. The 22 sessions reported in this paper were conducted using Claude Code versions 2.1.75 through 2.1.90 (March–April 2026). Future work includes evaluating a port to OpenAI Codex CLI to test whether the architectural principles (adversarial multi-agent dispatch, parametric generation with retrieval validation) transfer across LLM platforms.

Model versions. Throughout this paper, "Opus" refers to **Claude Opus 4.6** (`claude-opus-4-6`) and "Sonnet" refers to **Claude Sonnet 4.6** (`claude-sonnet-4-6`). Both models have a 1M token context window. Reliable knowledge cutoffs are May 2025 (Opus 4.6) and August 2025 (Sonnet 4.6), with training data extending to August 2025 and January 2026 respectively. Opus agents are configured at *maximum* effort (the highest reasoning investment); Sonnet agents at *high* effort (the maximum for Sonnet). These effort levels are pinned per agent in the configuration, overriding any session-level setting, to ensure reproducible quality. Cross-model validation uses **GPT-5.4 Pro** (OpenAI Responses API, March 2026) and **Gemini 3.1 Pro** (Google GenAI SDK, March 2026) via their respective APIs.

Reproducibility note. LLM outputs are non-deterministic: re-running the same `/discover` session with identical parameters produces different hypotheses. The evaluation in this paper reports results from specific sessions, not averaged across replications. The system's reproducibility claim is at the *architectural* level (the pipeline, agents, and prompts are fully open-source and can be re-executed), not at the *output* level. Temperature and sampling parameters are controlled by Claude Code's effort settings and are not independently configurable by the user.

Infrastructure. Agent dispatch uses Claude Code's standard sub-agent mechanism: the Orchestrator spawns each pipeline agent as an independent sub-agent with its own model, effort level, and tool permissions. Sub-agents communicate exclusively via files in `results/{session-id}/`, never via shared memory or direct messaging. Quality enforcement is implemented through SubagentStop hooks—deterministic Python scripts that validate every agent's output before allowing completion (exit code 2 = block, exit code 0 = approve). External data retrieval uses Model Context Protocol (MCP) servers for Semantic Scholar and PubMed, with web search as fallback. Approximate cost per session is $2–5 in API usage, with session duration of 15–45 minutes depending on adaptive cycle decisions.

3.2 Overview: Pipeline Flow

The pipeline proceeds as follows. In **Phase 1 (Exploration)**, the Scout generates 5–6 candidate cross-field targets using 10 strategies (Section 3.3). The Literature Scout verifies disjointness for all candidates and retrieves domain-specific literature. The Orchestrator narrows to 3 candidates, prioritizing citation-disjoint targets. The Target Evaluator adversarially challenges the 3 targets. The Orchestrator selects 1 target (subject to the disjointness hard constraint) and dispatches the Computational Validator for programmatic bridge verification.

In **Phase 2 (Generation & Critique)**, the Generator produces 6–8 hypotheses per cycle using parametric knowledge, literature context, and computational validation signals (Section 3.4). The Critic attacks each hypothesis with 9 adversarial vectors (Section 3.5). The Ranker scores survivors across 6 dimensions (Section 3.6). The Evolver applies genetic operations with a diversity constraint. This cycle repeats 1–3 times depending on adaptive quality thresholds (Section 3.7).

In **Phase 3 (Final Validation)**, the Quality Gate applies a 10-point rubric with per-claim grounding verification. Surviving hypotheses are independently validated by GPT-5.4 Pro and Gem-

ini 3.1 Pro. The Convergence Scanner and Dataset Evidence Miner search sources never consulted by the main pipeline (ClinicalTrials.gov, NIH Reporter, patents, HPA, GWAS Catalog, ChEMBL, UniProt, PDB) for independent evidence. The Session Analyst extracts meta-learning signals for future sessions.

3.3 Autonomous Target Selection (Scout)

The Scout is the agent that distinguishes MAGELLAN from systems requiring human-defined research objectives. Operating on Opus at maximum effort, it identifies promising cross-field bridges through 10 formalized strategies. These strategies were not designed a priori; they emerged from iterating on what produces high-quality targets. The first sessions used only 3 strategies (Swanson ABC, Structural Isomorphism, Tool Transfer); the remaining 7 were added as the Session Analyst identified underexplored modes of cross-disciplinary connection. The current set spans a spectrum from structured bibliometric methods (strategy 7) through creative elicitation (strategy 10):

1. **Recent Breakthrough Radiation** — Identifies implications of recent discoveries for non-obvious fields. In our evaluation, this strategy produced the lowest Quality Gate pass rate (13%, 1 session), suggesting that trending topics yield less novel connections.

2. **Anomaly Hunting** — Searches for reproducible but unexplained phenomena as hypothesis sources. First primary test (Session 018: Mpemba spectral relaxation × amyloid aggregation) produced 75% QG pass+conditional rate with mean composite 6.97.

3. **Converging Vocabularies** — Identifies fields that independently developed the same mathematical vocabulary or framework without mutual awareness. Highest pass rate in evaluation: 87.5% (Session 014: stochastic thermodynamics × bacterial cell-size control) and 75% (Session 017: extreme value theory × thermal proteomics).

4. **Tool Transfer Opportunities** — Identifies mature analytical or experimental tools in Field A that address unmet measurement needs in Field C. Combined pass rate across 2 sessions: ∼67%; Session 013 achieved 100% pass+conditional with mean composite 8.31—the highest of any session.

5. **Scale Bridging Gaps** — Identifies phenomena understood at one scale but absent at adjacent scales. One primary session (Session 005), 29% QG pass rate.

6. **Failed Paradigm Recycling** — Identifies ideas abandoned in one field that might succeed in a different context.

7. **Swanson ABC Bridging** — Systematic identification of disjoint literatures with shared intermediate concepts, directly implementing Swanson's original method. First primary test was confounded by a partially explored target; requires re-testing with verified disjoint targets.

8. **Contradiction Mining** — Active search for contradictions in the literature as hypothesis sources, inspired by FutureHouse's ContraCrow. When two papers in different fields make mutually exclusive claims, resolving the contradiction often reveals a non-trivial connection. Session 012 achieved 35.7% conditional pass rate.

9. **Structural Isomorphism Discovery** — Seeks fields sharing the same formal mathematical structure (equations, network topology, phase transition dynamics) with completely different physical substrates. The bridge concept is the mathematical object itself. Two primary sessions (Sessions 011 and 019) achieved 62.5% combined pass+conditional rate.

10. **Serendipity Through Random Encounter** — Picks a domain never explored in previous sessions, finds the most surprising recent discovery, and asks which distant field would be most transformed by knowing about it. The connection must cross at least 2 disciplinary boundaries. Mimics the serendipity of browsing a physical library.

Mandatory bridge concepts. Bridge concepts are required for every target, not only for the Swanson strategy. Even for Anomaly Hunting or Scale Bridging, the Scout must articulate a specific connection mechanism—molecules, pathways, mathematical structures, or physical principles. This forces structured reasoning and gives the Generator a richer starting point than a bare pair of fields.

Strategy diversification and exploration slot. Of the 3 selected targets, at least 2 must use different strategies, and at least 1 must use a strategy not employed in the last 2 sessions (verified against the persistent discovery log). This prevents strategic path-lock. Additionally, at least 1 target must use a strategy with fewer than 2 sessions of primary data (the *exploration slot*), preventing the system from always converging on the strategy with the best historical pass rate at the expense of more creative but less tested strategies.

Rotating creativity constraint. The Orchestrator assigns the Scout a different creativity constraint each session on a modular rotation of 5: cross-discipline bridge, mathematical/formal bridge, temporal gap exceeding 50 years, tool transfer, and unsolved problem. This forces exploration of territory the Scout would otherwise avoid.

TARGET QUALITY CHECK reflection. Before producing final output, the Scout performs a self-review: verifying bridge specificity, strategic diversity across the 3 targets, and non-obviousness. This reflection is one of six such loops in the system (Table 3).

3.4 Hypothesis Generation

The Generator operates on Opus at maximum effort, producing 6–8 hypotheses per cycle from three information sources: (1) parametric knowledge of both fields, (2) literature context from the Literature Scout (including full-text papers for the top 5–10 papers per field), and (3) computational validation signals from the Computational Validator (KEGG pathway cross-checks, STRING interaction scores, PubMed co-occurrence, and back-of-envelope physics calculations).

The parametric-generation paradigm. The most creative connections in MAGELLAN's output come from parametric reasoning—structural isomorphisms, bisociations, and multi-level abstractions that the model identifies from its training data. Web search validates these connections; it does not create them. This is a deliberate architectural choice: the Scout's 10 strategies are *elicitation mechanisms* for parametric knowledge, not search tools. The distinction matters because the most valuable UPK connections—the ones that Swanson originally identified—are precisely those that cannot be found by searching either literature in isolation.

Structured Relationship Map. Before generating hypotheses, the Generator builds an on-the-fly parametric knowledge graph for each field: listing 5–10 key relationships (X activates Y, W inhibits X, Y is analogous to V), searching for shared nodes between the two fields, identifying analogous relationships (A $\rightarrow$ B in Field A mirrors P $\rightarrow$ Q in Field C), and finding inverse relationships and missing links. This leverages the knowledge graph concept without external KG infrastructure: the LLM is the knowledge graph reasoner.

SELF-CRITIQUE loop. After generating hypotheses, the Generator performs a self-review: verifying mechanism specificity, checking for bridge duplication across hypotheses, identifying potential parametric error sources, and verifying each claim tagged as grounded. Claims are tagged as [GROUNDED] (literature-supported), [PARAMETRIC] (from model knowledge, requires verification), or [SPECULATIVE] (flagged as uncertain). The SELF-CRITIQUE verifies that [GROUNDED] tags are justified—this is the first of three claim-level verification steps (Generator, Critic, Quality Gate).

Bidirectional feedback. The Critic can write specific questions in the state JSON when a mechanism is too vague to attack properly. The Orchestrator forwards these `critic_questions` to the Generator in cycle 2, enabling indirect bidirectional feedback that preserves the centralized dispatch pattern.

3.5 Adversarial Validation Pipeline

The adversarial pipeline comprises the Critic, Quality Gate, and Cross-Model Validator. Together, these agents eliminate approximately 63% of generated hypotheses (the overall survival rate across 22 sessions is 37%).

3.5.1 The Critic: 9 Attack Vectors

The Critic operates on Opus at maximum effort. Its objective is genuinely adversarial: destroying weak hypotheses, not improving them. A kill rate of 30–50% is considered healthy; below 15% indicates insufficient adversarial pressure; a 0% kill rate triggers mandatory re-examination. The 9 attack vectors evolved incrementally: the first 6 were present from session 1; Hallucination-as-Novelty (vector 8) was added after the Si et al. findings on the ideation-execution gap, and Claim-Level Fact Verification (vector 9) was added after Session 004 revealed that citation hallucinations could survive mechanism-level attacks. The current vectors are:

1. **Novelty Kill** — Web search to verify whether the connection is already published. If the exact hypothesis (not merely the field pair) has been studied, the hypothesis is killed.
2. **Mechanism Kill** — Physical, chemical, or biological plausibility: energy scales, time constants, concentrations, compartment topology. This vector has produced the largest category of kills in our evaluation (15% of all kills are energy-scale mismatches; an additional 10% are quantitative impossibilities).
3. **Logic Kill** — Correlation passed off as causation, analogy confused with structural relationship, post-hoc reasoning.
4. **Falsifiability Kill** — If the hypothesis cannot be proven false, it is killed.
5. **Triviality Kill** — Would a PhD student in each field say "obviously"?
6. **Counter-Evidence Search** — Mandatory web search for contradictions and failures of the proposed mechanism.
7. **Groundedness Attack** — For every factual claim: is it from the literature (grounded), from parametric knowledge (verify with web search), or pure speculation (flag)? If >50% of claims are unverifiable, the hypothesis receives a significant downgrade.

8. **Hallucination-as-Novelty Check** — For hypotheses with high novelty scores: "Does it appear new because it is genuinely unexplored, or because it is wrong in non-obvious ways?" The Critic verifies via web search that the bridge mechanism exists independently of the hypothesis. If the novelty depends entirely on an unverifiable factual claim, the "novelty" is likely an artifact of incorrect parametric knowledge. This attack vector directly addresses the ideation-execution gap documented by Si et al. (Si et al., 2025a).

9. **Claim-Level Fact Verification** — Web search for *every individual* grounded claim. Verifies citation specificity (author, year, journal), directionality of effects, cellular compartment, protein properties. Citation hallucination or fabricated protein properties trigger automatic failure. This is the most critical attack vector: in our evaluation, citation-related errors account for approximately 6% of all kills (citation hallucination, citation misuse, partial citation hallucination).

META-CRITIQUE. After completing all attacks, the Critic performs a self-review: (1) calibrating its kill rate (is it too generous?), (2) for each surviving hypothesis, writing the strongest reason it should have been killed, and (3) verifying that web search was conducted for every hypothesis.

3.5.2 Quality Gate: 10-Point Rubric

The Quality Gate operates on Opus at maximum effort and applies a 10-point rubric covering mechanistic specificity, falsifiability, novelty, groundedness, internal consistency, and practical testability.[1] Critically, the Quality Gate *individually verifies every claim tagged as grounded*—the third and final claim-level verification step after the Generator's SELF-CRITIQUE and the Critic's fact verification. Citation hallucination or fabricated protein properties at this stage result in automatic failure, regardless of the hypothesis's other qualities.

The Quality Gate rejects approximately 60% of hypotheses that reach it. Its METAVALIDATION reflection verifies confidence in PASS verdicts, web search completeness, and the impact of any remaining unverifiable claims on the overall verdict.

Verdicts are PASS, CONDITIONAL_PASS (promising but with identified weaknesses), or FAIL. The authoritative verdicts are written to `quality-gate.json`; the Orchestrator creates `final.json` by reading this file from disk—never from conversational memory, which can be corrupted by context compression in long sessions (a bug discovered in Session 015).

3.5.3 Cross-Model Validation

After the Quality Gate, surviving hypotheses are automatically dispatched to two external frontier models via their APIs:

- **GPT-5.4 Pro** (OpenAI Responses API, reasoning effort: high, with web search and code interpreter) — Verifies novelty against current literature via web search. Checks arithmetic and quantitative claims computationally via code interpreter. Validates citations.

- **Gemini 3.1 Pro** (Google GenAI SDK, thinking level: HIGH, with code execution and Google Search grounding) — Verifies formal structural mappings computationally via code execution. Checks mathematical derivations. Validates literature claims via Google Search grounding.

[1] The complete Quality Gate rubric with scoring definitions, threshold examples, and verdict criteria is available in the repository at `.claude/agents/quality-gate.md`.

The Cross-Model Validator generates hypothesis-specific prompts, calls both APIs in parallel, and produces a consensus report identifying where the three models (Claude, GPT, Gemini) agree and diverge. This multi-model triangulation reduces the risk of a single model validating its own hallucinations—a concern when Claude generates hypotheses and Claude-based agents evaluate them.

Cross-model validation is non-blocking: API failures or missing keys do not change the session status. When API keys are absent, the system generates export files for manual validation.

3.6 Scoring

The Ranker evaluates each hypothesis across 6 dimensions with fixed, canonical weights (Table 4). These weights are immutable—bolded in the agent definition to prevent drift between cycles.

Design rationale. The 60% combined weight on Testability (20%), Groundedness (20%), and Mechanistic Specificity (20%) is deliberate. These three dimensions are the primary defense against the hallucination problem: a hypothesis can be creative and novel but must also be specific enough to test, grounded enough to believe, and mechanistically concrete enough to falsify. Novelty (15%) and Internal Consistency (15%) provide the remaining quality signal. Impact (10%) enters as a parallel signal—important for prioritization but never a substitute for quality.

Groundedness as anti-hallucination measure. The Groundedness dimension (20% weight) was introduced specifically to prevent the failure mode where fluent, creative hypotheses with fabricated factual claims score highly on other dimensions. Every hypothesis receives an integer Groundedness score from 1 to 10, where 10 indicates all mechanism components are supported by retrievable literature and 1 indicates pure speculation. This score is assessed independently by the Ranker and verified by the Quality Gate.

Cross-domain creativity bonus. After the weighted composite calculation, a +0.5 bonus is applied to hypotheses crossing 2 or more disciplinary boundaries (e.g., materials science → neuroscience, topology → developmental biology). This compensates for the systematic penalization from bio-centric retrieval infrastructure: non-biomedical hypotheses receive structurally lower scores on Testability and Groundedness because PubMed, KEGG, and STRING are bio-specific—not because the hypotheses are weaker. The bonus operates on the final composite; individual dimension weights remain immutable.

Impact-aware prioritization. Impact is decomposed into two sub-dimensions: Paradigm impact (5%, "opens a new field" = 10) and Translational impact (5%, "drug target or diagnostic" = 10, "purely academic" = 1). An Impact Potential Score (IPS) is computed from the Scout's initial estimate (40% weight) and the Convergence Scanner's translational signals (60% weight): $\text{IPS} = 0.4 \times \text{scout\_estimate} + 0.6 \times (\text{convergence\_signals}/3) \times 10$. The IPS is reported alongside the QG composite and Empirical Evidence Score but does not replace either.

Diversity check. After ranking, the Ranker examines the top-5 hypotheses for conceptual similarity: shared bridge mechanisms (redundant), same subfields (convergent), or same prediction type (monotonous). If 3 or more of the top-5 are conceptually similar, the highest-ranked is retained and the next dissimilar hypothesis is promoted. This addresses the diversity saturation problem documented by Si et al. (Si et al., 2024): LLM-generated ideas tend to cluster around a narrow region of the hypothesis space.

Elo tournament sanity check. After the linear ranking, the Ranker runs pairwise comparisons among the top-6 hypotheses (15 comparisons): "Which of these two would a researcher want to test first, and why?" The resulting Elo ranking is compared against the linear composite ranking. Discrepancies are diagnostic signals indicating implicit dimensions captured by direct comparison but missed by the 6-dimension weighted average. This is inspired by Google AI Co-Scientist (Gottweis et al., 2025), which uses Elo tournament as its primary ranking method. In MAGELLAN, it serves as a sanity check rather than the primary output, as we found the linear composite to be more transparent and auditable.

3.7 Adaptive Cycles and Meta-Learning

3.7.1 Adaptive Cycle Control

The Orchestrator has three decision points that adapt the pipeline to output quality, preventing both wasted compute on high-quality output and insufficient processing of low-quality output:

1. **Groundedness reinforcement** (after cycle 1 critique): If most hypotheses have low or speculative Groundedness, the Literature Scout is re-dispatched with targeted searches on the specific mechanisms that lack grounding. This additional literature feeds the Generator in cycle 2.
2. **Adaptive cycle decision** (after cycle 1 ranking):
   - Top-3 composite ≥ 7.0 AND diversity passed $\rightarrow$ *early complete*: skip cycle 2, proceed to Quality Gate.
   - Survival rate $< 30\%$ OR top-3 composite < 4.0 $\rightarrow$ *extended*: require cycle 2, consider cycle 3.
   - Otherwise $\rightarrow$ *standard*: normal cycle 2.
3. **Conditional Evolver skip** (cycle 2, after ranking): If top-3 composite ≥ 6.5, diversity is passed, and no hypotheses share bridges $\rightarrow$ skip the Evolver and proceed to the Quality Gate.

This adaptivity has a scaling property: a more capable model produces higher-quality output earlier in the pipeline, and the adaptive thresholds allow the system to terminate sooner without sacrificing quality.

3.7.2 Meta-Learning Across Sessions

The Session Analyst extracts three categories of meta-learning signals after each session:

Strategy performance. Which of the 10 Scout strategies produced hypotheses that survived the adversarial pipeline? Over 22 sessions, converging vocabularies achieved the highest pass rate (87.5% in Session 014, 75% in Session 017), followed by tool repurposing (100% pass+conditional in Session 013 with mean composite 8.31). Recent breakthrough radiation underperformed at 13%, suggesting trending topics yield less novel connections. These signals are written to `knowledge/meta-insights.md` and consulted by the Scout in future sessions.

Bridge type survival. Which types of mechanistic bridges survive adversarial evaluation? Computational and analytical tool transfers within life sciences showed the highest performance (3 PASS, 1 CONDITIONAL from 4 hypotheses in Session 013, mean composite 8.31). Physical law constraints (e.g., thermodynamic uncertainty relation as a hard bound on biological observables) showed 100% pass+conditional (7/7 in Session 014). Conversely, direct electromagnetic field effects (0/8 across Sessions 001 and 004) and quantum entanglement bridges (0/3 in Session 004) were universally killed due to energy-scale mismatches and decoherence at biological scales.

Kill pattern analysis. What are the recurring reasons for hypothesis failure? The dominant kill categories are: energy-scale mismatch (15% of all kills), quantitative impossibility including diffusion physics and force-below-threshold (14%), mechanism fabrication including wrong compartment or topology (9%), and substrate or condition mismatch (9%). These patterns inform both the Generator (which receives "avoid" guidelines) and the Scout (which deprioritizes target types that consistently produce killed hypotheses).

3.7.3 Disjointness Hard Constraint

A critical finding from our evaluation is the strong correlation between citation disjointness and hypothesis quality. Targets where the two fields have zero cross-field citation (classified as DISJOINT by the Literature Scout) achieved an 84% pass+conditional rate across 14 targets in 13 sessions. Partially explored targets (some existing cross-field literature) achieved only 30% conditional-only rate (1 session, with 0% outright PASS). Based on this evidence, the Orchestrator enforces a hard constraint: if DISJOINT targets with Target Evaluator score ≥ 5 exist, the system *never* selects a PARTIALLY_EXPLORED target.

An important nuance emerged from Sessions 015–016: partially explored *fields* can contain disjoint *bridges*. When a specific bridge (a particular measurement or mechanism) has ≤ 2 PubMed papers despite the fields being broadly overlapping, the target is classified as NEWLY_OPENED_PARTIALLY_EXPLORED and treated as functionally disjoint for hypothesis generation. Three such sessions achieved 100% QG pass+conditional rates.

3.8 State Management

State is split into a **slim coordination index** and **per-session results directories**:

- `state/session.json` — Approximately 3 KB containing only coordination state: current phase, cycle number, status, selected target, health counters, and progress timeline. This file *never* contains hypothesis content.
- `results/{session-id}/` — All session outputs: human-readable markdown (`*.md`) and structured phase data (`*.json`) in the same directory. Phase JSON files contain lightweight metadata (IDs, titles, scores, verdicts). Full hypothesis text lives in the markdown files.
- `state/dispatch-log.json` — Records every agent dispatch with timestamps, used for post-session verification that all required agents were invoked.

Design rationale. Agents receive the data they need via dispatch prompts from the Orchestrator—they never read state files directly. This design prevents two problems: (1) state bloat, where hypothesis content accumulates in a single file and consumes increasing context in later pipeline phases; and (2) stale reads, where an agent reads state that has been partially updated.

The Orchestrator reads authoritative outputs from disk (e.g., `quality-gate.json` for final verdicts) rather than from conversational memory, which can be corrupted by context compression in long sessions.

Robustness mechanisms. The pipeline must operate without human supervision. Three layers of robustness ensure this. *Guard logic in the Orchestrator*: conditional blocks after every phase verify output quality; the flow is always verify → retry → fallback → abort. *Blocking SubagentStop hooks*: per-agent hooks that block execution (exit code 2) when output is insufficient—e.g., the Scout hook blocks on 0 targets, the Generator hook blocks on < 3 hypotheses, and the Ranker hook blocks on output < 3 KB (preventing thin scoring without detailed justifications). *Session health classification*: every session terminates with an explicit status (SUCCESS, PARTIAL, DEGRADED, or FAILED) as the first line of the session summary, eliminating the possibility of silently empty output.

Prompt engineering. Agent prompts follow a GOAL / CONSTRAINTS / STRATEGIES structure: the goal is immutable, constraints are hard requirements, and strategies are advisory. This design scales with model capability: a more capable model finds better reasoning paths given goals and constraints, while the constraints maintain a quality floor regardless of model. Opus agents receive general instructions ("general instructions often produce better reasoning than prescriptive plans"); Sonnet agents receive more explicit step sequences. Few-shot examples are provided for the Generator (2 examples: strong and weak), Critic (1 complete attack), Ranker (1 scoring table), and Evolver (1 evolutionary operation).

4 Evaluation

4.1 Aggregate Results

The 22 sessions spanned a wide range of cross-disciplinary targets, from stochastic thermodynamics applied to bacterial cell-size control (S014) to percolation theory applied to tumor immune exclusion (S019), extreme value theory applied to thermal proteomics (S013), and Fisher information applied to plant gravitropism (S016). Target pairs were selected autonomously by the Scout in 16 sessions, with the remaining 6 specified by the user or curated for holdout validation. The targets deliberately cross terminological boundaries: a tumor immunologist would not typically encounter percolation thresholds, nor would a plant biologist recognize the Cramér-Rao bound as applicable to statolith dynamics.

Over these 22 sessions, MAGELLAN generated 273 hypotheses.[2] Of these, 102 (37.4%) survived the full adversarial pipeline with a verdict of PASS or CONDITIONAL_PASS. The Quality Gate rejected approximately 60% of hypotheses that reached it, consistent with our design goal that filtration, not generation, is the primary challenge.

Table 5 summarizes the aggregate statistics. The mean Quality Gate composite score for passing hypotheses was 7.1/10.0, with a range of 5.2–8.55. Sessions ranged from 7 to 15 hypotheses generated, with kill rates between 0% (Session 009, which produced only CONDITIONAL_PASS results) and 75% (Session 002). The adaptive cycle mechanism triggered early completion in 3 sessions (cycle 1 top-3 ≥ 7.0) and Evolver skip in 4 sessions (cycle 2 top-3 ≥ 6.5).

[2]All statistics in this paper reflect pipeline version as of April 2026. The public dashboard at `https://magellan-discover.ai` may show updated figures from subsequent sessions.

4.1.1 Strategy Performance

The Scout's 10 exploration strategies exhibited markedly different survival rates (Table 6). The strongest performers were *converging vocabularies* (87.5% PASS+COND rate across 2 sessions), which identifies fields using the same mathematical formalism without knowing it, and *tool repurposing* (67% combined, with Session 013 achieving 100%), which transfers analytical methods from one domain to another. *Anomaly hunting* (75% in its debut session) and *structural isomorphism* (62.5% across 2 sessions) also performed well.

At the bottom, *recent breakthrough radiation* achieved only 13% survival, suggesting that trending topics produce less novel cross-disciplinary connections—the "obvious" implications have typically been explored already. *Swanson ABC bridging*, the classical literature-based discovery method, produced 0% outright PASS (30% CONDITIONAL), though its single primary session was confounded by a PARTIALLY_EXPLORED target.

We caution that these rankings rest on small samples (1–3 primary sessions per strategy, 10–41 hypotheses each); binomial 95% confidence intervals are wide (e.g., 87.5% from 22 hypotheses corresponds to approximately ±14 percentage points). The rankings should be treated as suggestive hypotheses about strategy effectiveness rather than definitive estimates.

Key finding: mathematical constraints outperform analogies. The strongest strategies share a common structural feature: they transfer *mathematical constraints* (inequalities, conservation laws, universality theorems) rather than analogies or mechanistic parallels. When Field A contributes a theorem that *must* hold for any system of Field C's type, the resulting hypothesis has a distinctive epistemic property: the mathematical form is *guaranteed*, and the only testable variable is whether the biological parameters fall within the theorem's domain of applicability. This means the hypothesis is partially validated by construction—it cannot be wrong about the mathematics, only about the biology. By contrast, analogical bridges ("X in Field A resembles Y in Field C") are testable in both directions and empirically weaker.

This insight, extracted by the Session Analyst across multiple sessions, has been codified as a meta-learning heuristic: "Physical law as bridge > physical model as bridge." It is perhaps the most actionable methodological finding from the evaluation: researchers seeking cross-disciplinary connections should look for mathematical theorems that apply to systems they study, not just for surface similarities with other fields.

4.1.2 Bridge Type Survival

Bridge types—the structural form of the cross-disciplinary connection—predict survival rates more reliably than strategies (Table 7). Computational and analytical tool transfers within the life sciences achieved the highest performance (3 PASS, 1 COND from 4 hypotheses in Session 013, mean composite 8.31). Physical law constraints (e.g., the thermodynamic uncertainty relation applied to bacterial cell division) showed 100% PASS+COND (7/7). Indirect enzymatic cascades with named molecular participants showed ∼100% survival across 8+ hypotheses.

The failed bridge types share a common failure mode: *energy/force scale mismatch*. Direct electromagnetic field effects (0/8) fail because the proposed coupling energies are orders of magnitude below thermal noise at biological temperatures. Quantum entanglement bridges (0/3) fail because decoherence times in biological systems (∼femtoseconds) are incompatible with the timescales required for functional quantum effects. Direct force-on-chromatin bridges (0/2 in Session 016) fail because cytoskeletal forces, distributed across thousands of molecular contacts, produce per-element forces below the nucleosome unwrapping threshold (∼50 pN) by 3–4 orders of magnitude.

These patterns are now codified as pre-generation kill checks in the meta-learning knowledge base. New hypotheses proposing any of these bridge types are flagged before they consume pipeline resources.

4.1.3 Disjointness Analysis

The strongest predictor of hypothesis quality is *disjointness*—whether the target fields have zero mutual citation in the literature. Disjointness is operationalized via PubMed co-occurrence queries: for target fields A and C, the Literature Scout searches "`field_A AND field_C`" with field-specific MeSH terms and keyword variants. A target is classified DISJOINT if the query returns zero results across all variant queries, and PARTIALLY_EXPLORED if 1–10 results exist. Targets classified as DISJOINT achieved an 84% combined PASS+COND rate across 14 targets in 13 sessions. PARTIALLY_EXPLORED targets achieved only 30% (CONDITIONAL only, 0% outright PASS) in the single traditional case (Session 009). We caution that this operationalization has limitations: PubMed coverage is biology-centric, and fields connected through non-biomedical literature (e.g., physics preprints on arXiv) could be misclassified as disjoint.

This finding motivated the disjointness hard constraint: when DISJOINT targets with target evaluator scores ≥ 5 exist, the Orchestrator *never* selects a PARTIALLY_EXPLORED alternative. The constraint has been validated across 13 autonomous sessions.

An important nuance emerged from targeted sessions (S015–S016): PARTIALLY_EXPLORED *at the field level* can be functionally DISJOINT at the *bridge level*. When the broad fields overlap (e.g., mechanobiology and epigenomics) but the specific bridge mechanism is unstudied ($\leq$2 PubMed papers), hypothesis quality matches DISJOINT targets. This led to a refined two-level classification: field-level overlap and bridge-level novelty are assessed independently.

4.2 Validation Taxonomy

Before presenting the computational verifications, we distinguish four levels of validation for AI-generated hypotheses, in increasing order of evidential strength:

1. **Adversarial survival.** The hypothesis passed the full pipeline (Critic, Quality Gate, cross-model validation). This establishes internal consistency, mechanistic plausibility, and novelty—but not empirical truth. All 102 surviving hypotheses are at this level.

2. **Statistical analysis on public data.** A quantitative prediction is tested against existing datasets. The GEV/Meltome analysis (Section 4.3) is at this level: the primary prediction was falsified, though novel findings emerged.

3. **Mathematical derivation from published parameters.** A bound or prediction is derived from first principles using independently measured physical parameters. The CRB/gravitropism result (Section 4.4) is at this level: the derivation *is* the result—a mathematical consequence of published measurements, not a statistical hypothesis. What requires experimental testing are the *predictions* that follow from the bound (N-scaling, cytoskeletal inhibitor paradox), not the bound itself.

4. **Independent convergence evidence.** External sources—clinical trials, patents, independent publications—confirm the core mechanism without knowledge of the hypothesis. The percolation/immune exclusion hypothesis (Section 5.2) has convergence evidence at this level from three independent sources.

5. **Experimental validation.** Direct laboratory testing of the hypothesis. No MAGELLAN hypothesis has reached this level.

This taxonomy matters because "computationally verified" is not a single category. The CRB derivation is not "computationally plausible pending lab testing"—it is a valid physical bound. The GEV analysis, by contrast, was a quantitative test that the data did not support. Conflating these levels understates the strength of the former and overstates the latter.

4.3 Computational Verification I: GEV/Meltome Atlas

Session 013 (2026-03-27, autonomous, *tool repurposing* strategy) targeted the application of extreme value theory to the Meltome Atlas (Jarząb et al., 2020). Hypothesis C1-H1 (QG composite 7.85, PASS) predicted that the Generalized Extreme Value (GEV) shape parameter ξ, fitted to proteome-wide melting temperature (Tm) distributions, should correlate negatively with optimal growth temperature (OGT): thermophiles compress their lower Tm tail (more negative ξ, deeper into the Weibull domain) while psychrophiles maintain broader tails (ξ closer to zero).

Methodology. We loaded pre-computed Tm values from Jarzab et al. 2020 Supplementary Table S2 (MOESM4; PRIDE accession PXD011929). Quality filters retained only proteins with $R^2 \geq 0.8$ and converged curve fits, with Tm restricted to $[20°C, 100°C]$. One lysate dataset per species was selected to avoid confounds between cell and lysate preparations. GEV distributions were fitted via maximum likelihood estimation (`scipy.stats.genextreme`, which uses the sign convention $c = -\xi$; all reported ξ values are converted to the standard EVT convention where $\xi < 0$ corresponds to the Weibull domain), with bootstrap standard errors ($n = 1000$). We emphasize that the GEV is used here as a flexible three-parameter distributional family for descriptive fitting, not as an asymptotic limit theorem in the sense of the Fisher-Tippett-Gnedenko theorem (which would require block maxima construction from i.i.d. sequences). The application is analogous to fitting a log-normal distribution to income data without claiming a multiplicative central limit theorem. Spearman rank correlation tested ξ vs. OGT across 13 species. All code is publicly available in the verification directory of the repository.

Results. Table 8 presents the complete GEV fit results for all 13 species. The first notable finding is that *all* 13 species exhibit $\xi < 0$, placing them in the Weibull domain of the GEV family. This demonstrates that proteome Tm distributions are *universally bounded*—there exists a finite upper limit to protein thermal stability within each proteome. This is physically reasonable (amino acid chemistry imposes an upper bound on achievable Tm) but had not been formally demonstrated.

Goodness of fit. The KS test rejects the GEV model at $\alpha = 0.05$ for 6 of 13 species (46%), including *D. rerio*, *S. cerevisiae*, *H. sapiens*, *B. subtilis*, *E. coli*, and *O. antarctica*. For the large proteomes ($n > 1000$), this is partly expected: the KS test has high statistical power and can reject even adequate distributional approximations for minor deviations. We note that the standard KS null distribution assumes known (not estimated) parameters; with MLE-estimated parameters, the reported p-values are liberal. A Lilliefors-type parametric bootstrap would produce more conservative p-values. We retain the GEV framework because (a) the ξ estimates are stable under bootstrap resampling (Table 8, 95% CI column), and (b) the qualitative finding—universal $\xi < 0$—is robust under all bootstrap replicates, but acknowledge that the GEV is a descriptive approximation to the empirical Tm distribution, not an exact generative model. The KS p-values should be interpreted as approximate goodness-of-fit indicators rather than rigorous hypothesis test results.

The predicted correlation. The primary prediction—that ξ correlates negatively with OGT—is **not confirmed**. The Spearman rank correlation is $\rho = -0.136$ ($p = 0.658$), indicating no monotonic relationship. A Pearson correlation ($r = -0.628$, $p = 0.022$) appears significant but is entirely driven by a single outlier: *Thermus thermophilus* ($\xi = -2.374$).

The *T. thermophilus* artifact. The GEV fit for *T. thermophilus* produces $\mu = 95$°C—above the thermal proteome profiling (TPP) measurement ceiling of 90°C. This means the mode of the fitted distribution lies *outside the observable range*. The extremely negative ξ is an artifact of the GEV attempting to capture a severely left-censored distribution: the measurement window truncates the right side of the true Tm distribution, and the MLE compensates by pulling ξ to extreme negative values. Table 9 confirms this diagnosis: removing *T. thermophilus* eliminates all correlation ($\rho = +0.10$, $p = 0.75$).

MAGELLAN's contribution: novel findings from a falsified prediction. The primary prediction failed—but the failure is itself informative, and the analysis that led to it produced results that had no precedent in the literature. The key point is that *no researcher had applied extreme value theory to thermal proteomics data before this analysis*. MAGELLAN autonomously identified this cross-disciplinary connection (Session 013, Scout strategy: tool repurposing), and the resulting analysis—regardless of the specific correlation prediction—constitutes the first application of EVT to proteome-wide Tm distributions (confirmed via PubMed co-occurrence search: zero prior literature for "extreme value theory AND thermal proteome profiling" and 8 query variants).

This generated three novel findings:

1. **Universal Weibull-domain behavior across all three domains of life.** All 13 species, spanning Bacteria, Archaea, and Eukaryota with OGT from 15°C to 70°C, exhibit $\xi < 0$, placing them in the Weibull domain of the GEV family. In the language of the Fisher-Tippett-Gnedenko theorem (Fisher & Tippett, 1928; Gnedenko, 1943), proteome Tm distributions are *bounded above*—there exists a finite upper limit to protein thermal stability within each proteome. This is physically reasonable (amino acid chemistry constrains achievable Tm) but had not been formally demonstrated across the tree of life. We note the caveat that the TPP measurement ceiling (∼90°C) could contribute to universal negative ξ via right-censoring bias; disentangling biological bounds from measurement artifacts requires censoring-aware EVT methods.

2. **Identification of measurement censoring as the dominant confound in thermal proteomics.** The *T. thermophilus* anomaly ($\mu_{\text{GEV}} = 95$°C, above the 90°C measurement ceiling) reveals that standard TPP analysis produces severe artifacts for any species whose proteome thermal mode approaches the measurement window boundary. This is a methodological insight relevant to the entire thermal proteomics field, independent of the original hypothesis.

3. **Self-correcting hypothesis portfolio.** The censoring artifact was independently predicted by a companion hypothesis from the *same* MAGELLAN session (C1-H3: "Censored GEV Recovers the Invisible 20%"), which proposed applying censored maximum likelihood methods from flood frequency analysis to the TPP measurement window. The system generated both the prediction and its own diagnostic—demonstrating that multi-hypothesis generation creates a portfolio where hypotheses critique each other. Implementing censored GEV estimation (analogous to methods used for censored flood records in hydrology) constitutes the primary follow-up analysis.

Figure 1 shows ξ vs. OGT for all 13 species, with the *T. thermophilus* outlier clearly visible. Figure 2 shows representative Tm distributions with GEV fits for a mesophile (*E. coli*), a thermophile (*G. stearothermophilus*), and the artifact case (*T. thermophilus*).

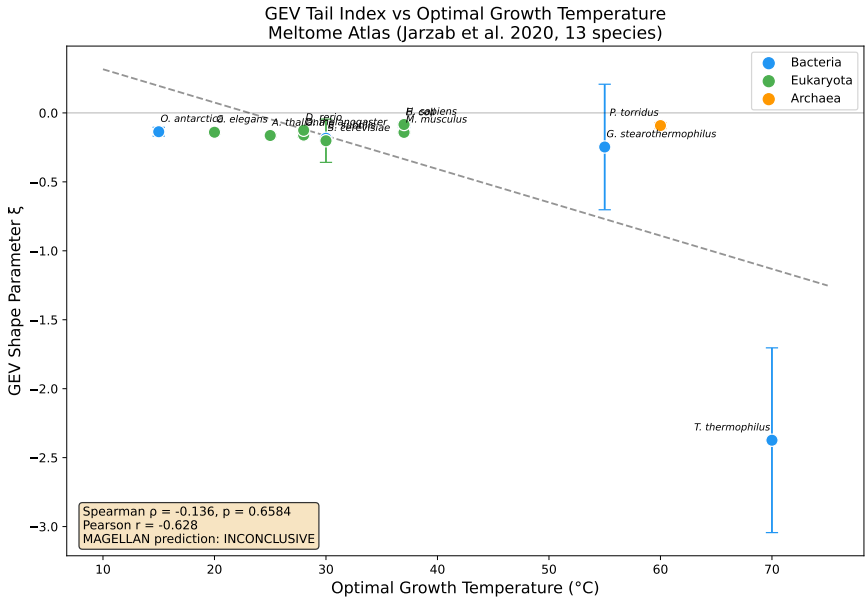

Figure 1: GEV shape parameter ξ vs. optimal growth temperature for 13 Meltome Atlas species. The extreme outlier (*T. thermophilus*, $\xi = -2.37$) is a measurement censoring artifact ($\mu_{\text{GEV}} = 95°\text{C}$ exceeds the TPP window of 30–90°C). Excluding it eliminates all correlation.

Assessment. This verification illustrates three aspects of MAGELLAN's output. First, hypotheses are *specific enough to falsify*: the prediction was quantitative, the dataset was public, and the test was unambiguous. Second, the act of connecting two previously unlinked fields—extreme value theory and thermal proteomics—has independent scientific value even when the specific prediction fails. The universal Weibull-domain finding and the measurement censoring diagnostic would each merit a short methods paper in bioinformatics; neither existed before MAGELLAN identified the connection. Third, the self-correcting portfolio (C1-H1 making the prediction, C1-H3 predicting its failure mode) suggests that multi-hypothesis generation is more valuable than generating a single "best" hypothesis, because the portfolio contains its own internal checks.

4.4 Computational Verification II: Cramér-Rao Bound for Gravitropism

Session 016 (2026-04-01, targeted, *mathematical bridge* creativity constraint) generated a hypothesis applying the Cramér-Rao bound (CRB) from statistical estimation theory to plant gravitropic sensing. The hypothesis scored 8.75 at Quality Gate (PASS) and was verified to have zero prior literature: 0 papers apply Fisher information or CRB to plant gravitropism, versus over 100 papers applying CRB to neural and animal sensory coding (Chauvet et al., 2016).

Physical setup. Plant gravitropic sensing relies on statoliths—starch-filled amyloplasts that sediment under gravity within columella cells at the root tip. Bérut et al. (Bérut et al., 2018) showed that statoliths behave as an active granular liquid with an effective temperature $T_{\text{eff}} \approx 10\times$ thermal,

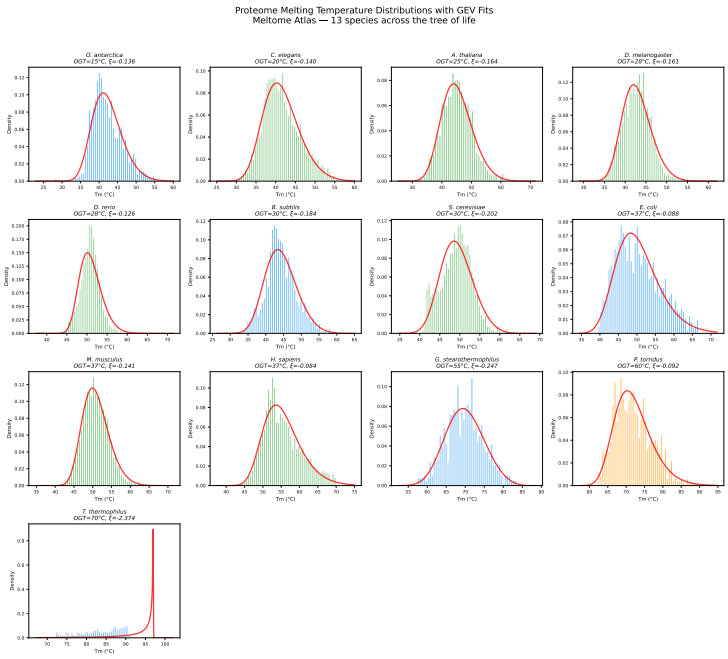

Figure 2: Proteome Tm distributions with GEV fits for three representative species. Note the right-truncation artifact in *T. thermophilus*, where the fitted μ (95°C) lies above the measurement ceiling (90°C).

due to cytoskeletal agitation. The key physical parameters are given in Table 10, all from published measurements.

Derivation. Consider N statoliths in a columella cell of half-width W, inclined at angle θ from vertical. Each statolith has mass $m = \frac{4}{3}\pi r^3 \Delta\rho$ and experiences a lateral gravitational potential component proportional to $\sin\theta$. At effective temperature T_{eff}, the lateral position distribution is a truncated exponential:

$$p(x \mid \theta) = \frac{\eta\, e^{-\eta x}}{1 - e^{-\eta W}}, \qquad \eta(\theta) = \frac{mg\sin\theta}{k_B T_{\text{eff}}} = \frac{\sin\theta}{\lambda} \tag{1}$$

where $\lambda = k_B T_{\text{eff}}/mg$ is the sedimentation length. In the sedimented regime ($\eta W = W\sin\theta/\lambda \gg 1$, which holds for all biologically relevant parameters at $\theta \gtrsim 1°$), the truncation correction is negligible, $\mathrm{Var}[x] \approx 1/\eta^2 = \lambda^2/\sin^2\theta$, and the Fisher information per statolith with respect to θ is:

$$I_1(\theta) = \left(\frac{\partial \eta}{\partial \theta}\right)^2 \mathrm{Var}[x] \approx \frac{\cos^2\theta}{\lambda^2} \cdot \frac{\lambda^2}{\sin^2\theta} = \cot^2\theta \tag{2}$$

Note that λ cancels: the Fisher information is dimensionless, as required for a parameter θ measured in radians. Near $\theta = 0$, the lateral Péclet number $\eta W \to 0$ and statoliths approach a uniform distribution over $[0, W]$ with $\mathrm{Var}[x] = W^2/12$, yielding a finite Fisher information $I_1(0) = W^2/(12\lambda^2)$; the full truncated-exponential model (used in our numerical code) handles this transition continuously.

The independence assumption deserves scrutiny: Bérut et al. showed that statoliths behave as an active granular liquid with collective avalanche dynamics, implying spatial correlations. However, positive correlations between statolith positions can only *reduce* the effective Fisher information (the independent case is the upper bound). Thus, if statoliths are correlated, the true CRB is *higher*

than our estimate, and plants would be operating even closer to the physical limit—strengthening rather than weakening the conclusion.

For N independent statoliths, the CRB on angular resolution is:

$$\sigma_\theta \geq \text{CRB}(\theta) = \frac{1}{\sqrt{N \cdot I_1(\theta)}} = \frac{\tan\theta}{\sqrt{N}} \tag{3}$$

Results. Table 11 presents the CRB across the full range of inclination angles for three parameter scenarios (optimistic: large statoliths, many per cell; mid-range; pessimistic: small statoliths, few per cell). At the standard experimental test angle of $\theta = 5°$, the CRB ranges from 0.79° to 2.37°. The observed plant angular resolution of 1°–5° (Chauvet et al., 2016) means that plants operate **1–6× above the fundamental physical limit**.

This result is **confirmed**: the CRB is a valid, non-trivial lower bound on plant angular resolution. The ratio of observed to theoretical limit (1–6×) is comparable to other biological sensory systems: photoreceptors operate 5–10× above the shot noise limit, and bacterial chemotaxis sensors operate 2–10× above their CRB (Berg & Purcell, 1977). This suggests a general principle: evolved biological sensors operate within roughly one order of magnitude of their fundamental physical limits.

N-scaling prediction. A direct corollary of Equation 3 is that angular resolution should scale as $\sigma_\theta \propto 1/\sqrt{N}$ with statolith count. This generates a specific, testable prediction: starchless mutants with reduced statolith numbers should show degraded angular resolution following a square-root law (Table 12).

Additional testable predictions. Beyond N-scaling, the CRB framework generates three further predictions: (1) Cytoskeletal inhibitors that reduce T_{eff} should *paradoxically improve* angular precision by reducing the noise floor against which the gravitational signal competes. (2) A nonlinear transition in gravitropic response should occur near $\theta \approx 0.3°$ where the lateral Péclet number approaches unity and the sedimented-regime approximation breaks down. (3) Species with larger statoliths (greater m, smaller λ) should have finer angular resolution at any given θ.

Novelty. This is the **first application of Fisher information to plant gravitropism**. Systematic searches across 8 query variants confirmed zero PubMed co-occurrence, versus over 100 papers applying CRB to neural and animal sensory coding. The gap is purely domain-specific: the mathematics is proven, the biology is measured, but no one has connected them. This is the type of "undiscovered public knowledge" (Swanson, 1986) that MAGELLAN is designed to find.

Figure 3 shows the CRB as a function of inclination angle for three parameter regimes, compared to the observed resolution band. Figure 4 places plant gravitropism in context with other biological sensing systems operating near physical limits.

Two verifications, two outcomes. The pairing of a partially falsified prediction (GEV/Meltome, Section 4.3) with a confirmed one (CRB/gravitropism) is itself informative. It demonstrates three properties of MAGELLAN's output: hypotheses are *specific enough to falsify* (the GEV prediction was quantitative and testable), *novel enough to contribute* (even the falsified prediction produced the first EVT analysis of thermal proteomics), and *precise enough to confirm* (the CRB prediction was validated from published parameters alone).

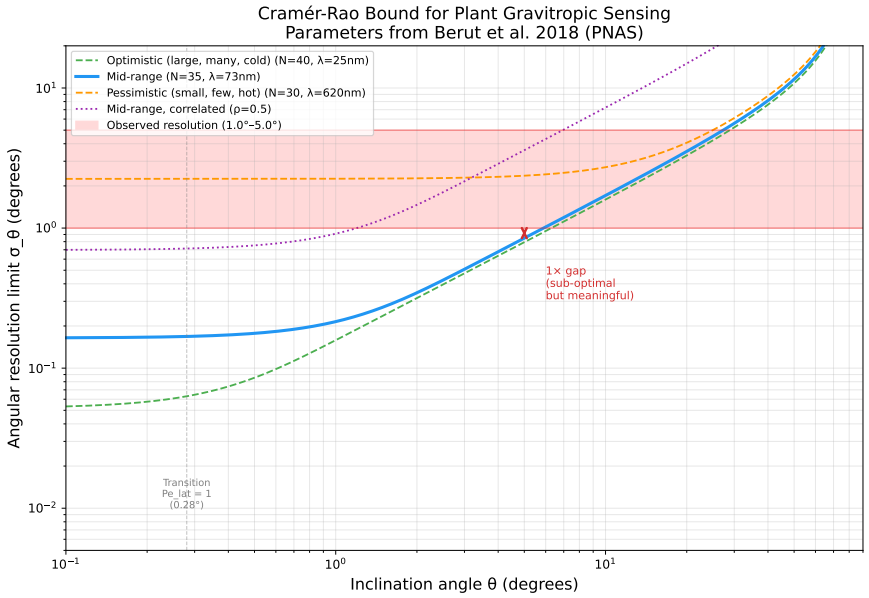

Figure 3: Cramér-Rao bound for plant gravitropic angular resolution as a function of inclination angle θ. Three parameter regimes are shown (optimistic, mid-range, pessimistic). The red band indicates observed plant resolution (1°–5°, Chauvet et al. 2016). Plants operate 1–6× above the fundamental physical limit at the standard test angle ($\theta = 5°$).

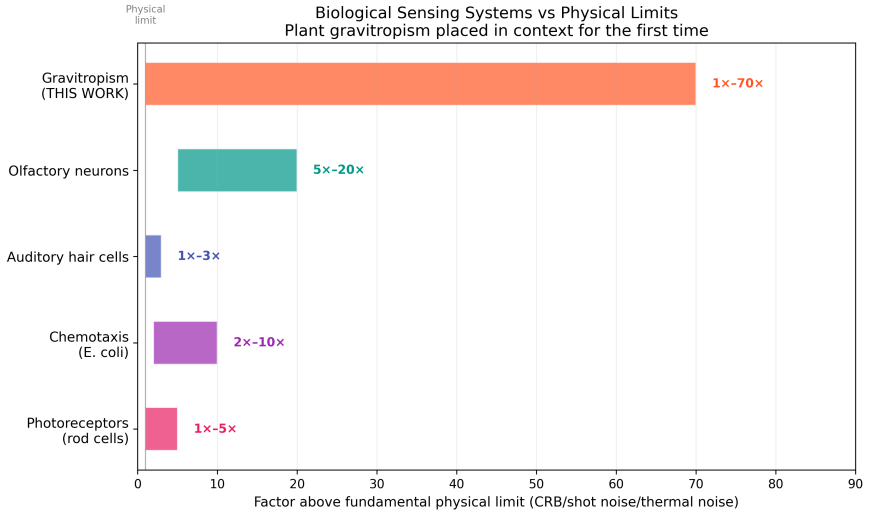

Figure 4: Biological sensing systems compared to their fundamental physical limits. Plant gravitropism (this work) operates 1–70× above the Cramér-Rao bound, comparable to photoreceptors and chemotaxis sensors. This is the first time gravitropism has been placed in this context.

Qualitative sophistication. It is worth pausing to consider what these verifications represent in terms of cross-disciplinary reasoning depth. The CRB derivation required simultaneous knowledge of (a) the Fisher information formalism from statistical estimation theory, (b) the physics of Boltzmann-distributed particles in gravitational potentials, (c) the specific biology of statolith dynamics in plant columella cells, and (d) the measured parameters from Bérut et al. 2018 on active granular liquids. The resulting derivation is not a qualitative analogy ("statoliths are like sensory receptors") but a quantitative bound with an elegant property: the sedimentation length λ cancels from the Fisher information, yielding a dimensionless result that depends only on the tilt angle and statolith count. A human researcher arriving at this result would need training in both statistical physics and plant biology—precisely the kind of cross-disciplinary expertise that Swanson's UPK framework identifies as the bottleneck. Similarly, the percolation hypothesis does not merely observe that tumors have dense ECM; it applies the Weinrib-Halperin theory for correlated disorder to derive quantitative drug synergy predictions from universality class exponents—a level of mathematical specificity that goes well beyond "field A resembles field C."

4.5 Cross-Model Validation

After the Quality Gate, surviving hypotheses are independently evaluated by two external frontier models: GPT-5.4 Pro (OpenAI, with web search and code interpreter enabled) and Gemini 3.1 Pro (Google, with code execution and Google Search grounding enabled). The Cross-Model Validator agent generates hypothesis-specific validation prompts and dispatches them via API calls, producing a consensus report.

The rationale is adversarial diversity: if a hypothesis survives criticism from three independently trained models (Claude Opus 4.6 generating and critiquing, GPT-5.4 Pro empirically validating, Gemini 3.1 Pro structurally analyzing), the remaining failure modes are more likely to be genuinely subtle rather than artifacts of a single model's blind spots. The three models have different training data, different reasoning strategies, and different tool access patterns.

In practice, the cross-model validation has identified three categories of disagreement:

1. **Novelty assessment divergence**: GPT-5.4, with access to more recent web results, occasionally identifies relevant recent papers that Claude's pipeline missed. This has caused post-hoc downgrade of novelty scores in 2 sessions.

2. **Quantitative verification**: GPT-5.4's code interpreter enables independent recalculation of numerical predictions (e.g., Péclet numbers, dissipation rates). In Session 014, this caught a discrepancy in entropy production estimates.

3. **Structural analysis**: Gemini's code execution capability has been used to verify mathematical derivations (e.g., Fisher information calculations, percolation exponent relationships).

Cross-model validation is non-blocking: API failures or unavailability do not change session status. When API keys are not configured, the system generates self-contained export files that can be manually pasted into GPT or Gemini interfaces.

4.6 Holdout Validation

To test whether MAGELLAN can independently rediscover known scientific findings, we curated three holdout targets from post-2025 publications (Table 13). Each target represents a confirmed cross-disciplinary discovery published after the system's design was finalized. The validation protocol is: (1) present only the two fields ("Field A $\times$ Field C") without revealing the known mechanism,

(2) run the standard pipeline, (3) check for contamination (did the pipeline find the answer paper?), and (4) score mechanism similarity between MAGELLAN's output and the known discovery.

Holdout-001 (Grippin et al. (Grippin et al., 2025), *Nature* 2025) demonstrated that mRNA SARS-CoV-2 vaccines sensitize tumors to immune checkpoint blockade via type I interferon-mediated CD8+ T cell priming—an unexpected connection between vaccinology and cancer immunotherapy with a 5-fold improvement in 3-year overall survival for low PD-L1 tumors. Holdout-002 (DeCasien et al. (DeCasien et al., 2026), *PNAS* 2026) showed that gut microbiota from large-brained primate species upregulate brain oxidative phosphorylation genes in germ-free mice—the first experimental link between microbiome composition and brain evolution. Holdout-003 (Cosgrove et al. (Cosgrove et al., 2025), *Science* 2025) discovered "mechanoenhancers," a class of genomic regulatory elements activated by extracellular matrix stiffness, with direct implications for fibrosis.

Contamination issue. Holdout-003 presented a contamination challenge: Sessions 015 and 016 had already targeted mechanobiology × epigenomics before the holdout was curated. The pipeline's literature retrieval found the Cosgrove et al. 2025 paper during these sessions, making it impossible to test uncontaminated rediscovery for this target. This is a structural limitation of holdout validation for an autonomous system—the system may discover the relevant field pair before the holdout test is administered.

Holdouts 001 and 002 remain uncontaminated and available for future validation runs. The full holdout protocol includes five verdicts: GENUINE_REDISCOVERY (mechanism independently found), PARTIAL_REDISCOVERY (related mechanism, different specifics), ADJACENT_DISCOVERY (same fields, different connection), CONTAMINATED (answer paper found), and MISSED (no relevant output).

4.7 Failure Analysis

Of the ∼171 hypotheses that did *not* survive the adversarial pipeline, we classified failure modes from the Session Analyst's meta-learning outputs. Table 14 presents the dominant kill patterns.

Why EM fields and quantum bridges always fail. Direct electromagnetic field effects (0/8) and quantum entanglement bridges (0/3) represent the pipeline's most consistent failure mode. The mechanism is always the same: the proposed coupling energy is orders of magnitude below k_BT at biological temperatures. For EM fields, typical proposed interaction energies ($\sim \mu$eV) are 10^3–$10^4\times$ below thermal noise. For quantum coherence, decoherence times in warm, wet biological environments (∼fs) are $10^{12}\times$ shorter than required for functional quantum effects. These bridge types are now pre-screened out by meta-learning heuristics.

What the Critic catches vs. what the Quality Gate catches. The Critic and Quality Gate serve complementary roles. The Critic excels at *mechanism-level* kills: wrong compartment topology (T6SS fires inward, not outward), physically impossible spatial gradients (Péclet number $\ll 1$), and counter-evidence from literature search. Its kill rate of 30–50% is by design. The Quality Gate excels at *claim-level* verification: it individually web-searches every [GROUNDED] claim and catches citation hallucinations (fabricated DOIs, wrong journal attributions, papers cited for the opposite of their actual conclusion). The citation hallucination rate of ∼2–3% of grounded claims is low but nonzero—the Quality Gate caught a fabricated citation in Session 013 ("Mateus et al. 2020, Science 367:eaaz5268" was a conflation of Tan 2018 and Mateus 2020) and a fabricated first author in Session 018 ("Avanzini et al. 2026" when the actual first author was Summer).

Emergent kill patterns. Several kill patterns emerged only after multiple sessions and were codified into pre-generation checks:

- **Force-per-contact check** (Session 016): For mechanobiology hypotheses proposing direct force on chromatin, the total cytoskeletal force (∼10–100 pN) divides across ∼100,000+ molecular contacts, yielding per-element forces of ∼0.001 pN—3–4 orders of magnitude below nucleosome unwrapping thresholds.
- **Data-structural form check** (Session 017): Mathematical methods require specific data structures (temporal ordering for extremal indices, sufficient density for trend fitting). Cross-sectional proteome data lacks the temporal ordering required by several EVT methods.
- **Symmetry constraint pre-check** (Session 018): Standard protein Markov state models enforce detailed balance by construction, making the transition matrix normal. Proposing non-normality measures for standard MSMs is structurally impossible.

5 Case Studies

The computational verifications (Sections 4.3–4.4) tested specific predictions against data. Here we present two passing hypotheses in their full reasoning chain—from target selection through mechanism specification to falsification test design—to illustrate the *depth* of cross-disciplinary reasoning the system produces. We selected these two because they represent the highest-performing bridge types identified by the meta-learning analysis: *physical law as constraint* (Case Study 1: the thermodynamic uncertainty relation applied to bacterial cell division) and *structural isomorphism* (Case Study 2: percolation theory applied to tumor immune exclusion). Both emerged from fully autonomous sessions where the Scout chose the target, the fields had zero mutual citation, and the resulting hypotheses include quantitative predictions with specific laboratory falsification protocols.

5.1 Case Study 1: FtsZ GTPase Dissipation Identifies the Precision Bottleneck in Bacterial Cell Division

Session context. Session S014 (autonomous, *converging vocabularies* strategy) targeted the thermodynamic uncertainty relation (TUR) from stochastic thermodynamics and the bacterial adder model of cell size homeostasis. Disjointness: 0.96 (zero PubMed papers bridging TUR and adder model).

Hypothesis. The bacterial cell cycle involves two major entropy-producing molecular currents: DnaA-ATP hydrolysis at the origin of replication ($\Sigma_{\text{DnaA}} \approx 11 \times 20\, k_B T = 220\, k_B T$ per initiation) and FtsZ-GTP hydrolysis in the Z-ring during division ($\Sigma_{\text{FtsZ}} \approx 300 \times 6.5$ GTP/min $\times$ 15 min $\times$ $15\, k_B T \approx 405{,}000\, k_B T$ per division). The entropy production ratio is ∼1,840×. By the TUR, the minimum achievable coefficient of variation (CV) scales as $\text{CV}^2 \geq 2/\Sigma$. Thus DnaA counting sets a TUR floor of CV $\geq 9.5\%$, while FtsZ sets CV $\geq 0.22\%$.

The precision bottleneck is definitively at *initiation* (DnaA), not at *division* (FtsZ). FtsZ's enormous entropy production serves a mechanical function (constriction force), not an informational one (precision timing).

Quality Gate verdict. PASS, composite 7.90. All key parameters independently verified: FtsZ $k_{\text{cat}} \approx 8$/min (Romberg & Mitchison, 2004), FtsZ treadmilling (Bisson-Filho et al., 2017), $N_{\text{eff}} = 11$

DnaA binding sites (McGarry et al., 2004). The entropy production calculation is robust: even at the lowest Z-ring occupancy (200 monomers), the FtsZ/DnaA ratio exceeds 800×.

Falsification test. FtsZ84 (temperature-sensitive GTPase mutant, ∼10% activity) at semi-permissive temperature: CV of added size should *not* increase significantly. *dnaA46* (temperature-sensitive initiation mutant) at semi-permissive temperature: CV should increase by 15–30%. The *asymmetric* response identifies the precision bottleneck. Both mutants are standard laboratory alleles available in stock centers.

Significance. This hypothesis transforms a qualitative question ("Where is precision limiting in the cell cycle?") into a quantitative prediction from first principles. The TUR is a mathematical inequality that *must* hold for any dissipative counting process; the hypothesis tests whether the biological system operates near one bound or the other. This is the "physical law as bridge" pattern identified by the Session Analyst as the highest-performing bridge type.

5.2 Case Study 2: Percolation Theory Predicts LOX/Anti-TGF-β Synergy in Immune-Excluded Tumors

Session context. Session S019 (autonomous, *structural isomorphism* strategy) targeted the application of percolation threshold theory to T cell infiltration in solid tumors. Disjointness: 0.95 (zero prior literature on percolation phase transitions applied to tumor immune exclusion).

Hypothesis. The extracellular matrix (ECM) of solid tumors can be modeled as a 3D bond percolation network, where LOX-mediated collagen crosslinks define bond occupation probability p. Below a critical threshold $p_c \approx 0.22$ (for Voronoi tessellation with coordination number $z \sim 6$–8), a spanning cluster of connected pores permits T cell migration (immune-hot tumor). Above p_c, no spanning cluster exists (immune-cold tumor). The bond open/closed threshold is calibrated to the nuclear cross-section constraint of 4 μm^2 (Wolf et al., 2013).

TGF-β–mediated integrin activation creates spatially *correlated* collagen crosslink density with a correlation length of 40–60 μm around cancer-associated fibroblasts (CAFs). Using the Weinrib-Halperin theory for exponentially correlated disorder (Weinrib & Halperin, 1983), this correlation shifts p_c upward by +0.035 to +0.075 above the random-percolation threshold, making the tumor ECM *harder to percolate* than a random collagen network with the same mean crosslink density.

Quantitative prediction. LOX inhibition (BAPN or PXS-5505) raises p by +0.10–0.15, while anti-TGF-β (galunisertib) lowers p_c by 0.035–0.075. The combination achieves a $p - p_c$ margin of ∼0.17 versus ∼0.12 for BAPN alone or ∼0.05 for anti-TGF-β alone. Since infiltration scales as $P_\infty \sim (p - p_c)^{0.417}$ (3D percolation universality class), the combination produces $P_\infty \sim 0.57$ versus 0.47 (BAPN alone) or 0.30 (anti-TGF-β alone). This is super-additive synergy calculable from percolation physics.

Quality Gate verdict. CONDITIONAL_PASS, composite 7.6. Grounded claims verified: Weinrib & Halperin (1983) (confirmed), Nicolas-Boluda et al. (2021) (confirmed), TGFB1-LOX STRING interaction score 0.623 (confirmed). Condition: verify the active-particle correction to p_c (T cells are not passive random walkers; Péclet number ∼3 may modify the universality class).

Convergence evidence. The Convergence Scanner found striking independent confirmation: (1) NCT05109052, a Phase 1b/2 trial of PXS-5505 (pan-LOX inhibitor) combined with atezolizumab and bevacizumab for hepatocellular carcinoma, whose rationale explicitly states "improved survival when combined with systemic therapy through increased intratumoral drug delivery and enhanced host anti-tumor immunity." (2) Patent WO2024003558A1 (Institute of Cancer Research, 2023) states "LOX reduction reduces ECM content and tumor stiffness leading to improved T cell migration and increased efficacy of anti-PD-1 blockade." (3) A 2026 *Science Immunology* paper (PMID 41860994) independently demonstrated that collagen network *topology*—not bulk stiffness—governs T cell localization, which is precisely the central premise of the percolation framework.

Neither the clinical trial nor the patent uses percolation theory, but both operationalize the core mechanism. The percolation framework adds *quantitative predictions* (specific p_c thresholds, drug combination synergy magnitudes, universality class exponents) that the existing qualitative understanding lacks.

6 Discussion and Limitations

6.1 What MAGELLAN Can and Cannot Do

MAGELLAN demonstrates that adversarial multi-agent systems can autonomously identify cross-disciplinary connections that are specific, mechanistically detailed, and sometimes computationally verifiable. The 37% survival rate across an adversarial pipeline with independent cross-model validation suggests that the system is neither too permissive (random hypotheses would survive at $<5\%$) nor too conservative (the meta-learning system identifies and prunes entire bridge categories). The two computational verifications—one confirmed, one partially falsified—demonstrate that the output is empirically meaningful.

A dimension that aggregate statistics do not capture is the *qualitative sophistication* of individual hypotheses. The surviving hypotheses are not shallow analogies between fields ("X is like Y"). They involve quantitative bounds derived from physical theorems (CRB, TUR), phase transition predictions from universality classes (percolation), and specific drug synergy calculations from first principles. Each requires fluent reasoning across two or more disciplines that share no common terminology—precisely the cross-field integration that Swanson identified as the bottleneck in 1986 and that has only widened since. Whether this reflects genuine "understanding" of both fields or a sophisticated pattern-matching over training data is an open question; what is not in question is that the *outputs* are at a level of specificity and mathematical precision that makes them independently evaluable by domain experts and, in the CRB case, independently confirmable from published data alone.

However, the system has fundamental limitations that must be stated honestly.

6.2 No Experimental Validation

The most important limitation is that **no MAGELLAN hypothesis has been tested in a laboratory**. The computational verifications in Sections 4.3 and 4.4 use published data and first-principles calculations. The convergence evidence for the percolation hypothesis (Section 5.2) includes a Phase 1b/2 clinical trial testing the core mechanism, but this trial was designed independently of MAGELLAN.

We note, however, that the validation taxonomy (Section 4.2) matters here. The CRB derivation is not a statistical hypothesis awaiting laboratory confirmation—it is a mathematical consequence of measured physical parameters. The bound itself is established; what requires experimental testing

are the *predictions* it generates (statolith count scaling, cytoskeletal inhibitor effects, the nonlinear transition regime). Similarly, the percolation hypothesis has three independent convergence signals (clinical trial, patent, peer-reviewed publication) that confirm the core mechanism from different angles. These results occupy a different evidential position from "computationally plausible but untested."

This places MAGELLAN in a fundamentally different position from Google's AI Co-Scientist (Gottweis et al., 2025), which reported three experimentally validated discoveries (KIRA6 for AML, vorinostat for hepatic fibrosis, cf-PICIs for bacterial gene transfer). Google had wet-lab collaborators who could test predictions within weeks; MAGELLAN has none. The distance between "computationally plausible" and "experimentally confirmed" is the central gap in our evidence. The system publishes all hypotheses with test protocols and cost estimates precisely to invite domain experts to close this gap.

6.3 Life Sciences Bias

The pipeline exhibits three coupled biases toward the life sciences. At the retrieval level, PubMed, KEGG, and STRING are all bio-specific; no equivalent MCP servers exist for arXiv or INSPIRE-HEP. At the scoring level, 60% of the composite weight (Testability + Groundedness + Mechanistic Specificity) favors experimental sciences with structured databases. At the format level, few-shot examples in agent prompts use molecular and pathway language.

These biases produce a measurable score asymmetry. Session S-targeted-015 (prime numbers $\times$ black holes) achieved 100% QG pass+cond rate but 0% outright PASS: all three hypotheses received CONDITIONAL_PASS because the math-physics domain lacks existing measurement datasets for immediate verification. A physics hypothesis with composite score 5.5 may be qualitatively equivalent to a biomedical hypothesis with score 7.0. The cross-domain creativity bonus (+0.5 for hypotheses crossing 2+ disciplinary boundaries) partially compensates but does not eliminate this asymmetry.

6.4 Measurement Censoring as Lesson

The GEV/Meltome verification provides a general lesson about computational verification of AI-generated hypotheses. The prediction appeared to have weak support ($r = -0.63$, $p = 0.02$) until careful examination revealed that the entire signal was an artifact of measurement censoring in a single species. This is a failure mode specific to *computationally verifiable* hypotheses: the verification can produce a false positive if the data's limitations are not understood.

MAGELLAN's own pipeline anticipated this: a companion hypothesis from the same session (C1-H3) independently predicted that TPP measurement censoring would create artifacts for thermophilic species. The fact that the system generated both the flawed prediction and its own correction speaks to the value of multi-hypothesis generation: the portfolio approach produces hypotheses that critique each other.

6.5 The Generation-Validation Gap: A Shifted Bottleneck

One of the more striking observations from operating MAGELLAN is the asymmetry between generation and validation costs. A single `/discover` session (15–45 minutes, $2–5 of API cost) produces 7–15 hypotheses, of which 2–6 survive adversarial review. Computationally verifying a single hypothesis (the GEV and CRB analyses) required 1–2 days of focused work each. Experimental verification of even the simplest hypothesis would require a domain expert with cross-disciplinary training.

This asymmetry reveals a structural shift: **the bottleneck in AI-assisted scientific discovery is no longer hypothesis generation—it is domain expertise to evaluate the output**. For forty years since Swanson, the challenge was to *find* cross-disciplinary connections. MAGELLAN can now produce them faster than they can be evaluated, at negligible cost, across arbitrary field pairs. The new challenge is triage: which of the 102 surviving hypotheses are worth a domain expert's time? The system's scoring, ranking, convergence evidence, and validation taxonomy are designed to assist this triage, but they cannot replace the judgment of a scientist who understands both fields. This reframing—from "how do we find connections?" to "how do we prioritize AI-generated connections for human evaluation?"—may be the most practically important implication of this work.

6.6 Missing Ablations

We have not conducted ablation studies to measure the marginal contribution of individual pipeline components (e.g., removing the Critic, disabling cross-model validation, using a single LLM instead of the multi-agent architecture). The 37% survival rate is a property of the *complete system*; we cannot currently attribute it to any specific component. This limits our ability to recommend which architectural elements are essential versus incidental. Future work should include controlled ablations with a specific protocol: (1) removing the Critic entirely (measuring how many Quality Gate FAILs would have been caught earlier), (2) disabling cross-model validation (measuring whether GPT/Gemini disagreements correlate with downstream quality), (3) replacing the multi-agent architecture with a single-LLM chain-of-thought approach (measuring whether the agent specialization architecture contributes beyond simple prompting), and (4) disabling meta-learning heuristics (measuring the cumulative value of session-over-session learning). The primary metrics would be survival rate, composite score distribution, and—ideally—blinded expert quality assessments.

6.7 Comparison to Prior Systems

Among published AI discovery systems, Google's AI Co-Scientist (Gottweis et al., 2025) is the most directly comparable. Key differences: (1) Google requires a scientist-in-the-loop to frame the research question; MAGELLAN's Scout autonomously decides where to look. (2) Google has wet-lab collaborators; MAGELLAN has none. (3) Google reported 3 validated discoveries; MAGELLAN reports 0 validated, 2 computationally verified, and 102 adversarially surviving. (4) Google is proprietary; MAGELLAN is fully open-source.

FutureHouse's Robin/Kosmos achieved 79.4% on structured agentic tasks (Mitchener et al., 2025) but only 57.9% on novel synthesis—suggesting that AI systems perform well on tasks with clear evaluation criteria but struggle with genuinely open-ended discovery. MAGELLAN's 37% survival rate on a *self-imposed* adversarial pipeline is not directly comparable (our pipeline may be more or less stringent than FutureHouse's evaluation), but the principle is similar: generation is easier than validation.

6.8 Citation Hallucination

Despite multiple verification layers (Generator self-critique, Critic claim-level verification, Quality Gate per-claim web search), approximately 2–3% of grounded claims contain citation errors. These are predominantly *conflations* rather than fabrications: the system correctly recalls a finding but misattributes it (wrong first author, wrong journal, wrong year). The most common pattern is correct venue and year with a fabricated first author for very recent papers (<6 months old).

This rate is low but consequential: a single fabricated citation triggers automatic FAIL at the Quality Gate. The meta-learning system has codified this into mandatory pre-generation verification rules (e.g., verify first author names for papers published in the past 6 months via web search before citing).

6.9 Broader Implications

If AI systems can routinely find genuine cross-field connections that humans have missed, the implications extend beyond individual discoveries to the structure of the scientific process itself.

Scale. The scale advantage is stark: MAGELLAN searches 10 cross-disciplinary targets per session, across any pair of scientific fields, in under an hour. A human researcher building equivalent cross-field knowledge—reading the literatures of both percolation theory and tumor immunology, or both estimation theory and plant gravitropism—would require years. The system does not replace the depth of domain expertise; it replaces the *breadth of reading* that no individual can achieve. In a single week, it can survey more cross-disciplinary pairs than a research group explores in a career.

A new collaboration model. This suggests a mode of human-AI scientific collaboration that differs from the "AI as research assistant" paradigm of most current systems. Rather than helping a scientist work faster within their field, MAGELLAN presents scientists with connections *from outside their field*—connections they would never encounter through normal reading, conference attendance, or collaboration. The scientist's role shifts from generating hypotheses to *evaluating* them: a plant physiologist receives a Fisher information derivation and asks, "Does this bound make sense given what I know about statolith dynamics?" This leverages what humans do best (deep domain judgment) and what AI does best (broad cross-domain pattern recognition).

Risk. The risk is also clear: fluent, specific, well-cited hypotheses that are *wrong* could consume scarce experimental resources. The adversarial pipeline is designed to minimize this risk, but a 37% survival rate means that 63% of generated hypotheses are eliminated internally. Of the survivors, some will be wrong in ways that the pipeline cannot detect without experimental data. The validation taxonomy, convergence evidence, and triage infrastructure are designed to help domain experts allocate their attention efficiently—but the final judgment must remain human.

6.10 Ethical Considerations

MAGELLAN's approach to responsible disclosure involves two principles:

1. **CC0 public domain licensing for autonomous discoveries.** All hypotheses generated in fully autonomous mode (`/discover` without arguments) are released under CC0 1.0, placing them in the public domain. This prevents any party—including us—from claiming intellectual property over AI-generated scientific hypotheses. Guided-mode discoveries (where a user provides domain context) are licensed CC-BY 4.0.

2. **Full transparency.** All hypotheses, including rejected ones, are published with their complete adversarial pipeline history (Critic attacks, Quality Gate verdicts, cross-model reports). Failures are as informative as successes: they reveal what *does not* work and why.

The system does not currently address dual-use risks (e.g., hypotheses about pathogen virulence mechanisms, toxin engineering, or biosecurity-sensitive targets). This is a limitation of the current

design; the pipeline has no content filter for potentially dangerous applications. Possible mitigations for future versions include keyword-based pre-screening of Scout targets against curated risk ontologies, domain expert review gates for flagged hypotheses before publication, and output-level content moderation. We note that the open-source nature of the system makes such safeguards advisory rather than enforceable—a tension inherent to transparent AI science tools.

7 Conclusion

MAGELLAN demonstrates that adversarial multi-agent systems running frontier language models can autonomously generate cross-disciplinary scientific hypotheses that are specific, testable, and empirically meaningful. Over 22 sessions, the system produced 273 hypotheses, of which 102 (37%) survived an adversarial pipeline including 9-vector criticism, claim-level fact verification, 10-point quality gate review, and independent evaluation by GPT-5.4 Pro and Gemini 3.1 Pro.

Computational verification on public data produced two outcomes: a partially falsified prediction (GEV tail index vs. growth temperature, revealing measurement censoring artifacts but producing the first extreme-value-theory analysis of thermal proteomics) and a confirmed prediction (Cramér-Rao bound for plant gravitropic sensing, showing plants operate 1–6$\times$ above the fundamental physical limit—the first application of Fisher information to plant gravity perception). Both analyses had zero prior literature.

The system's meta-learning reveals reliable patterns: cross-disciplinary connections based on mathematical constraints (conservation laws, inequalities, universality theorems) outperform those based on analogies or direct physical effects. Truly disjoint field pairs produce substantially better hypotheses than partially explored ones (84% vs. 30% survival). Certain bridge types (direct EM field effects, quantum entanglement) fail universally and can be pre-screened.

The bottleneck is no longer hypothesis generation. An autonomous system can produce specific, falsifiable, adversarially reviewed cross-disciplinary hypotheses faster than they can be experimentally tested. The missing piece is domain expertise: scientists in thermal proteomics, plant physiology, tumor immunology, bacterial cell biology, and dozens of other fields could evaluate whether the surviving hypotheses merit laboratory investigation. We have released all code, hypotheses, and methodology under Apache 2.0 and CC0 specifically to invite this evaluation. The hypotheses are available at `https://magellan-discover.ai/discoveries` and the source code at `https://github.com/kakashi-ventures/magellan-cli`.

The question MAGELLAN poses is not whether AI can replace scientists—it cannot—but whether it can systematically surface the cross-field connections that no individual scientist has the breadth to see. The evidence goes beyond survival statistics: the system autonomously derived a physical bound for plant gravitropism that no researcher in either statistical physics or plant biology had produced, connected percolation theory to tumor immunology in a way that three independent sources (clinical trial, patent, peer-reviewed paper) subsequently confirmed the core mechanism, and identified a precision bottleneck in bacterial cell division from a thermodynamic inequality. These are not analogies; they are quantitative, falsifiable scientific hypotheses that can be evaluated on their merits. Twenty-two sessions suggest that the answer is a cautious yes—and the results are publicly available for domain experts to judge.

Acknowledgments

This work was conducted without external funding. The MAGELLAN pipeline runs on Claude Code (Anthropic) and uses APIs from OpenAI (GPT-5.4 Pro) and Google (Gemini 3.1 Pro) for cross-

model validation. The author thanks the open-source and scientific communities whose published data (Meltome Atlas, PRIDE, PubMed) made the computational verifications possible. Claude Code was used as both the execution platform and a collaborative tool during paper preparation.

The author is grateful to the team at Kakashi Venture Accelerator (KVA) for supporting the testing and iteration of the MAGELLAN framework, and to his co-founder Federico Bottino (CEO of KVA) for the constant encouragement to pursue ambitious projects. The author dedicates this work to the memory of his mother, Loretta, who nurtured his curiosity and love for science from an early age. Finally, he thanks Carolina for her patience and support through the many sleepless nights that MAGELLAN required.

References

Swanson, D.R. (1986). Undiscovered public knowledge. *The Library Quarterly*, 56(2), 103–118.

Swanson, D.R. (1988). Migraine and magnesium: eleven neglected connections. *Perspectives in Biology and Medicine*, 31(4), 526–557.

Tenopir, C. et al. (2009). Electronic journals and changes in scholarly article seeking and reading patterns. *Aslib Proceedings*, 61(1), 5–32.

Rein, D. et al. (2023). GPQA: A graduate-level Google-proof Q&A benchmark. *arXiv preprint arXiv:2311.12022*.

Ginkgo Bioworks (2026). Cell-free protein synthesis optimization via GPT-5 collaboration. *Ginkgo Technical Report*.

Gottweis, J. et al. (2025). Towards an AI co-scientist. *Google DeepMind Technical Report*.

DeepMind (2025). Aletheia: Solving open mathematical problems with AI. *Google DeepMind Technical Report*.

Ji, Z. et al. (2023). Survey of hallucination in natural language generation. *ACM Computing Surveys*, 55(12), 1–38.

OpenAI (2025). FrontierScience-Research benchmark results. *OpenAI Technical Report*.

Si, C. et al. (2025). Can LLMs generate novel research ideas? A large-scale human study with 100+ NLP researchers. *ICLR 2025*.

Si, C. & Hashimoto, T. (2025). The ideation-execution gap: Execution outcomes of LLM-generated versus human research ideas. *arXiv preprint arXiv:2506.20803*.

Si, C. et al. (2024). Can LLMs generate diverse ideas? Measuring and improving idea diversity in LLM-generated scientific research ideas. *arXiv preprint arXiv:2410.13185*.

Smalheiser, N.R. (2009). Literature-based discovery: Beyond the ABCs. *Journal of the American Society for Information Science and Technology*, 63(2), 218–224.

Hristovski, D. et al. (2006). Using literature-based discovery to identify disease candidate genes. *International Journal of Medical Informatics*, 75(12), 879–889.

Ghafarollahi, A. & Buehler, M.J. (2024). SciAgents: Automating scientific discovery through multi-agent intelligent graph reasoning. *arXiv preprint arXiv:2409.05556*.

Mitchener, L. et al. (2025). Kosmos: An AI scientist for autonomous discovery. *arXiv preprint arXiv:2511.02824*.

Lu, C. et al. (2024). The AI Scientist: Towards fully automated open-ended scientific discovery. *ICLR 2025*.

Huang, K. et al. (2025). Automated hypothesis validation with agentic sequential falsifications. *International Conference on Machine Learning (ICML 2025)*. arXiv:2502.09858.

Swanson, K. et al. (2024). Virtual Lab: AI agents design new SARS-CoV-2 nanobodies with experimental validation. *arXiv preprint arXiv:2407.00510*.

Yang, B. et al. (2024). MOOSE-Chem: Large language models for rediscovering unseen chemistry scientific hypotheses. *ICLR 2025*.

Xiong, R. et al. (2025). TruthHypo: Truthful hypothesis generation with LLMs. *IJCAI 2025*.

Jarząb, A. et al. (2020). Meltome atlas—thermal proteome stability across the tree of life. *Nature Methods*, 17(5), 495–503. doi:10.1038/s41592-020-0801-4.

Bérut, A. et al. (2018). Gravisensors in plant cells behave like an active granular liquid. *PNAS*, 115(20), 5123–5128.

Chauvet, H. et al. (2016). Inclination not force is sensed by plants during shoot gravitropism. *Scientific Reports*, 6, 35431.

Berg, H.C. & Purcell, E.M. (1977). Physics of chemoreception. *Biophysical Journal*, 20(2), 193–219.

Kawamoto, N. & Morita, M.T. (2022). Gravity sensing and responses in the coordination of the shoot gravitropic setpoint angle. *New Phytologist*, 236, 1445–1460.

Fisher, R.A. & Tippett, L.H.C. (1928). Limiting forms of the frequency distribution of the largest or smallest member of a sample. *Mathematical Proceedings of the Cambridge Philosophical Society*, 24(2), 180–190.

Gnedenko, B.V. (1943). Sur la distribution limitée du terme maximum d'une série aléatoire. *Annals of Mathematics*, 44(3), 423–453.

Barato, A.C. & Seifert, U. (2015). Thermodynamic uncertainty relation for biomolecular processes. *Physical Review Letters*, 114(15), 158101.

Grippin, A.J., Marconi, C., Copling, S. et al. (2025). mRNA vaccines sensitize tumors to immune checkpoint blockade. *Nature*, 647(8089), 488–497. doi:10.1038/s41586-025-08795-1.

DeCasien, A.R., Aronoff, J.E., Mallott, E.K. et al. (2026). Gut microbiota from large-brained primates upregulate brain oxidative phosphorylation genes. *Proceedings of the National Academy of Sciences*, 123(2), e2426232122. doi:10.1073/pnas.2426232122.

Cosgrove, B.D., Bounds, L.R., Taylor, C.K. et al. (2025). Mechanoenhancers: genomic regulatory elements activated by extracellular matrix stiffness. *Science*, 390(6778), eadl1988. doi:10.1126/science.adl1988.

Romberg, L. & Mitchison, T.J. (2004). Assembly dynamics of the bacterial cell division protein FtsZ: Poised at the edge of stability. *Biochemistry*, 43(1), 282–288.

Bisson-Filho, A.W. et al. (2017). Treadmilling by FtsZ filaments drives peptidoglycan synthesis and bacterial cell division. *Science*, 355(6326), 739–743.

McGarry, K.C. et al. (2004). Two discriminatory binding sites in the *Escherichia coli* replication origin are required for DNA strand opening by initiator DnaA-ATP. *Proceedings of the National Academy of Sciences*, 101(9), 2811–2816.

Wolf, K. et al. (2013). Physical limits of cell migration: Control by ECM space and nuclear deformation and tuning by proteolysis and traction force. *Journal of Cell Biology*, 201(7), 1069–1084.

Nicolas-Boluda, A. et al. (2021). Tumor stiffening reversion through collagen crosslinking inhibition improves T cell migration and anti-PD-1 treatment. *eLife*, 10, e58688.

Weinrib, A. & Halperin, B.I. (1983). Critical phenomena in systems with long-range-correlated quenched disorder. *Physical Review B*, 27(1), 413–427.

DeepMind (2025). AlphaEvolve: A Gemini-powered coding agent for designing advanced algorithms. *Google DeepMind Technical Report*.

Schmidgall, S. et al. (2025). Agent Laboratory: Using LLM agents as research assistants. *arXiv preprint arXiv:2501.04227*.

Li, J. et al. (2025). A survey of AI scientists: Toward a six-stage scientific research paradigm. *arXiv preprint arXiv:2510.23045*.

Phan, L. et al. (2025). Humanity's Last Exam. *Nature*, 638, 1092–1097.

Majumder, B.P. et al. (2024). DiscoveryBench: Towards data-driven discovery with large language models. *NeurIPS 2024*.

Liu, J. et al. (2025). ResearchBench: Benchmarking LLMs in scientific discovery via inspiration-driven research. *arXiv preprint arXiv:2503.21370*.

Table 2: Agent architecture. "Opus" = Claude Opus 4.6 (`claude-opus-4-6`, max effort); "Sonnet" = Claude Sonnet 4.6 (`claude-sonnet-4-6`, high effort). Model assignment principle: Opus for deep cross-disciplinary reasoning; Sonnet for structured, search-intensive tasks. See Section 3.1 for full version details.

Agent	**Model**	**Role**
Scout	Opus	Target selection via 10 strategies; bridge concepts; strategy diversification; exploration slot; rotating creativity constraint; TARGET QUALITY CHECK reflection
Target Evaluator	Opus	Adversarial challenge on 4 axes: popularity bias, vagueness, structural impossibility, local optima
Literature Scout	Sonnet	MCP-first retrieval (Semantic Scholar, PubMed); full-text papers; disjointness verification; RETRIEVAL QUALITY CHECK reflection
Comp. Validator	Sonnet	Programmatic bridge verification: KEGG pathways, STRING interactions, PubMed co-occurrence, back-of-envelope physics
Generator	Opus	Hypotheses from parametric knowledge + literature context + computational validation; Structured Relationship Map; bisociation; SELF-CRITIQUE
Critic	Opus	9 adversarial attack vectors including claim-level fact verification; META-CRITIQUE reflection; writes `critic_questions` for cycle 2
Ranker	Sonnet	6-dimension weighted scoring; per-hypothesis table; diversity check; Elo tournament sanity check; cross-domain creativity bonus
Evolver	Sonnet	Genetic operations with diversity constraint; EVOLUTION QUALITY CHECK reflection; conditionally skippable
Quality Gate	Opus	10-point rubric; web novelty check; per-claim grounding verification; META-VALIDATION reflection
Session Analyst	Sonnet	Post-pipeline meta-learning: strategy performance, kill patterns, bridge type analysis → persistent knowledge base
Cross-Model Val.	Sonnet	Dispatches to GPT-5.4 Pro + Gemini 3.1 Pro APIs for independent validation; generates consensus report
Convergence Scan.	Sonnet	Searches ClinicalTrials.gov, NIH Reporter, patents for independent convergence signals
Dataset Evidence	Sonnet	Queries HPA, GWAS Catalog, ChEMBL, UniProt, PDB to verify specific molecular claims
Holdout Eval.	Opus	Compares output against known post-cutoff discoveries; contamination check + mechanism similarity scoring
Orchestrator	Opus	Pure dispatcher: guard logic, adaptive cycles, session health, meta-learning (no WebSearch/WebFetch)

Table 3: Reflection loops across the pipeline. Each agent performs a structured self-review before producing final output. External evaluation (SubagentStop hooks, Ranker minimum-size gates) prevents reflection from degenerating into self-congratulation.

Agent	**Reflection Name**	**What It Verifies**
Generator	SELF-CRITIQUE	Mechanism specificity, bridge duplication, parametric error sources, claim-level grounding
Critic	META-CRITIQUE	Kill rate calibration, strongest reason to kill each survivor, web search completeness
Scout	TARGET QUALITY CHECK	Bridge specificity, strategic diversity, non-obviousness
Quality Gate	META-VALIDATION	Confidence in PASS verdicts, web search completeness, impact of unverifiable claims
Literature Scout	RETRIEVAL QUALITY CHECK	MCP completeness, paper count per field, gap analysis specificity
Evolver	EVOLUTION QUALITY CHECK	Genuine improvement over parent, bridge duplication, crossover coherence

Table 4: Scoring dimensions and weights. The weights are canonical and immutable. The 60% combined weight on Testability, Groundedness, and Mechanistic Specificity reflects the system's structural optimization for life sciences, where these dimensions are most reliably assessable.

Dimension	**Weight**	**Description**
Novelty	15%	Is the connection unexplored? Requires web search verification, not self-assessment.
Mechanistic Specificity	20%	How concrete is the proposed mechanism? Named molecules, quantified parameters, and specified pathways score higher than vague analogies.
Testability	20%	Can the hypothesis be verified with existing methods or public data? Includes assessment of required resources and timeline.
Groundedness	20%	Are the hypothesis components supported by retrievable evidence? Integer 1–10. Prevents fluent hallucinations from scoring high.
Internal Consistency	15%	Are the claims internally coherent? Are quantitative predictions consistent with stated parameters?
Impact	10%	Decomposed into Paradigm (5%) and Translational (5%). Paradigm: how much does it change understanding if true? Translational: how directly does it suggest a real-world application?

Table 5: Aggregate pipeline statistics across 22 sessions.

Metric	Value
Total sessions	22
Fully autonomous (Scout)	16
Targeted (user-specified)	5
Holdout validation	1
Total hypotheses generated	273
Survived adversarial pipeline (PASS + COND)	102 (37.4%)
Outright PASS	∼42
CONDITIONAL_PASS	∼60
Quality Gate rejection rate	∼60%
Mean QG composite (passing)	7.1 / 10.0
Citation hallucination rate	∼2–3% of grounded claims
Sessions with early completion	3
Sessions with Evolver skip	4

Table 6: Scout strategy performance ranked by QG pass rate (PASS + CONDITIONAL_PASS). Only strategies with ≥1 primary session shown.

Strategy	Primary sessions	Hyps gen.	QG pass+cond	Avg composite
Converging vocabularies	2 (S014, S017)	22	87.5%	7.34
Anomaly hunting	1 (S018)	15	75%	6.97
Tool repurposing	2 (S010, S013)	24	∼67%	7.27
Structural isomorphism	2 (S011, S019)	16	62.5%	∼6.9
Network gap analysis	3 (S006–S008)	41	39%	6.92
Contradiction mining	1 (S012)	14	35.7%	6.70
Scale bridging	1 (S005)	14	29%	6.75
Recent breakthrough	1 (S004)	15	13%	∼6.0
Swanson ABC bridging	1 (S009)	10	30% (COND only)	5.87

Table 7: Bridge type survival rates. Top: consistently successful types. Bottom: consistently killed types.

Bridge type	Used	QG pass+cond	Score range
Successful bridge types			
Analytical tool transfer (life sci.)	4	4 (100%)	8.15–8.55
Physical law constraint (TUR)	7	7 (100%)	5.2–8.3
Indirect enzymatic cascade	8+	6+ (∼100%)	7.0–8.5
Mathematical topology	3	3 (100%)	∼8.0
Thermodynamic displacement	1	1 (100%)	8.1
Sequential enzymatic temporal gate	2	2 (100%)	7.5–7.8
Killed bridge types			
Direct EM field effects	8	0 (0%)	—
Quantum entanglement	3	0 (0%)	—
Mechanism fabrication (wrong compartment)	2	0 (0%)	—
Direct force on chromatin	2	0 (0%)	—
Spatial gradient (Pe $\ll$ 1)	2	0 (0%)	—

Table 8: GEV fit parameters for Meltome Atlas species, ordered by optimal growth temperature. All species show $\xi < 0$ (Weibull domain). μ = location, σ = scale, ξ = shape. KS = Kolmogorov-Smirnov goodness-of-fit p-value.

Species	**Domain**	**OGT**	n	ξ	**95% CI**	μ (°C)	**KS** p
O. antarctica	Bacteria	15	1264	−0.137	[−0.19, −0.06]	40.6	0.032
C. elegans	Eukaryota	20	3220	−0.140	[−0.16, −0.12]	39.6	0.180
A. thaliana	Eukaryota	25	2381	−0.164	[−0.19, −0.14]	43.1	0.072
D. melanogaster	Eukaryota	28	1646	−0.161	[−0.19, −0.14]	41.5	0.070
D. rerio	Eukaryota	28	3548	−0.126	[−0.15, −0.11]	49.8	0.000
B. subtilis	Bacteria	30	1471	−0.184	[−0.21, −0.16]	42.6	0.002
S. cerevisiae	Eukaryota	30	1938	−0.202	[−0.22, −0.18]	47.7	0.000
E. coli	Bacteria	37	1727	−0.088	[−0.12, −0.05]	47.9	0.006
M. musculus	Eukaryota	37	5347	−0.141	[−0.16, −0.13]	49.4	0.076
H. sapiens	Eukaryota	37	4562	−0.084	[−0.10, −0.07]	53.2	0.000
G. stearotherm.	Bacteria	55	716	−0.247	[−2.45, −0.21]	68.0	0.904
P. torridus	Archaea	60	896	−0.092	[−0.14, −0.05]	69.9	0.266
T. thermophilus	Bacteria	70	826	−2.374	[−3.26, −0.53]	95.0	0.000

Table 9: Spearman and Pearson correlations of ξ vs. OGT across subsets. The apparent Pearson signal disappears when the measurement-censored *T. thermophilus* is excluded.

Subset	n	**Spearman** ρ	**Pearson** r	**Pearson** p
All 13 species	13	−0.136	−0.628	0.022
Excl. *T. thermophilus*	12	+0.098	−0.067	0.837
Excl. both thermophiles	11	+0.145	+0.033	0.923
Mesophiles only (20–37°C)	8	+0.190	+0.119	0.779

Table 10: Physical parameters for the CRB derivation, all from Bérut et al. 2018 (Bérut et al., 2018) unless noted.

Parameter	**Value**	**Source**
Statolith radius r	2–4 μm	Confocal microscopy
Statoliths per cell N	30–40	Direct count
T_{eff}	10× thermal (≈2950 K)	Avalanche dynamics
$\Delta\rho$ (starch − cytoplasm)	300–500 kg/m^3	Standard values
Sedimentation length $\lambda = k_B T_{\text{eff}}/mg$	∼73 nm	Derived
Péclet number Pe $= L/\lambda$	∼340	Gravity $\gg$ noise
Columella cell half-width W	5–10 μm	Confocal microscopy
Observed angular resolution	1°–5°	Chauvet et al. 2016

Table 11: Cramér-Rao bound for gravitropic angular resolution vs. inclination angle. Three parameter scenarios span the published range. Observed plant resolution is 1°–5°.

θ (°)	**CRB optimistic**	**CRB mid**	**CRB pessimistic**
0.1	0.053°	0.165°	2.245°
0.5	0.085°	0.177°	2.247°
1	0.158°	0.215°	2.250°
2	0.316°	0.345°	2.265°
5	0.793°	0.847°	2.365°
10	1.597°	1.708°	2.719°
20	3.297°	3.525°	4.066°
45	9.059°	9.685°	10.468°

Table 12: Predicted angular resolution vs. statolith count N, at $\theta = 5°$ (mid-range parameters). Testable with starchless mutant lines.

N	**CRB (°)**	**Predicted obs. (×3 above CRB)**
5	2.24	6.7
10	1.59	4.8
20	1.12	3.4
35	0.85	2.5
40	0.79	2.4

Table 13: Holdout validation targets. Three confirmed post-2025 cross-disciplinary discoveries.

ID	**Field A**	**Field C**	**Key paper**	**Journal**
001	mRNA vaccinology	Immuno-oncology	Grippin et al. 2025	*Nature*
002	Gut microbiology	Primate brain evolution	DeCasien et al. 2026	*PNAS*
003	Mechanobiology (ECM)	Epigenomics (enhancers)	Cosgrove et al. 2025	*Science*

Table 14: Hypothesis kill patterns across 22 sessions. Percentages are approximate due to overlapping categories.

Kill pattern	**Count (%)**	**Representative session**
Energy/force scale mismatch	18 (11%)	S001, S004, S016
Quantitative impossibility	13 (8%)	S005, S007, S014
Substrate/condition mismatch	8 (5%)	S005
Mechanism fabrication (wrong compartment)	8 (5%)	S013, S014
Classical explanation sufficiency	6 (4%)	S001, S002
Mechanism fabrication (no pathway)	5 (3%)	S002, S006
Thermodynamic impossibility	4 (2%)	S005, S007
Citation hallucination	5 (3%)	S004, S018, S019
Mathematical invalidity	3 (2%)	S002
Binding affinity too weak	3 (2%)	S012
Time-scale mismatch	1 (<1%)	S016
Logic kill (internal contradiction)	1 (<1%)	S014